






Research Article

Analysis of Volterra Integrodifferential Equations with the Fractal-Fractional Differential Operator

Kamran ¹, Aisha Subhan ¹, Kamal Shah,^{2,3} Suhad Subhi Aiadi ², Nabil Mlaiki ²
and Fahad M. Alotaibi ⁴

¹Department of Mathematics, Islamia College Peshawar, Peshawar, Khyber Pakhtunkhwa, Pakistan

²Department of Mathematics and Sciences, Prince Sultan University, P.O. Box 66833, Riyadh 11586, Saudi Arabia

³Department of Computer Science and Mathematics, Lebanese American University, Byblos, Lebanon

⁴Department of Information Systems, Faculty of Computing and Information Technology (FCIT), King Abdulaziz University, Jeddah 34025, Saudi Arabia

Correspondence should be addressed to Kamran; kamran.maths@icp.edu.pk and Nabil Mlaiki; nmlaiki@psu.edu.sa

Received 13 December 2022; Revised 5 May 2023; Accepted 13 May 2023; Published 9 November 2023

Academic Editor: Abdellatif Ben Makhlouf

Copyright © 2023 Kamran et al. This is an open access article distributed under the Creative Commons Attribution License, which permits unrestricted use, distribution, and reproduction in any medium, provided the original work is properly cited.

In this paper, a class of integrodifferential equations with the Caputo fractal-fractional derivative is considered. We study the exact and numerical solutions of the said problem with a fractal-fractional differential operator. The abovementioned operator is arising widely in the mathematical modeling of various physical and biological problems. In our scheme, first, the integrodifferential equation with the fractal-fractional differential operator is converted to an integrodifferential equation with the Riemann–Liouville differential operator. Additionally, the obtained integrodifferential equation is then converted to the equivalent integrodifferential equation involving the Caputo differential operator. Then, we convert the integrodifferential equation under the Caputo differential operator using the Laplace transform to an algebraic equation in the Laplace space. Finally, we convert the obtained solution from the Laplace space into the real domain. Moreover, we utilize two techniques which include analytic inversion and numerical inversion. For numerical inversion of the Laplace transforms, we have to evaluate five methods. Extensive results are presented. Furthermore, for numerical illustration of the abovementioned methods, we consider three problems to demonstrate our results.

1. Introduction

Fractional calculus (FC) is considered as the generalization of classical calculus. The origin of FC can be traced back to the end of the seventeenth century, the time when Newton and Leibniz developed the foundation of differential and integral calculus. We can say that the integer order calculus describes the local dynamics, while FC describes the global dynamics of a physical system. In FC, the major fractional differential and integral operators are the Riemann–Liouville (RL), the Caputo, the Caputo–Fabrizio (CF), and the Atangana–Baleanu (AB) fractional operator. The difference between these operators is their kernel [1]. The Caputo's fractional operator is based on the power law, the CF operator is based on the exponential decay law, and the AB

operator is based on the Mittag–Liffler law. Mathematicians commonly utilize the RL derivative; however, this approach is unsuitable for real world physical problems. Fractional differentiation and integration are understood in Caputo's sense because of its applicability to real world physical problems. FC is an emerging field in mathematics with deep application in all related fields of science and engineering [2, 3]. The research community use fractional calculus to obtain important results and generalizations from modeling of complex systems. These complex systems are characterized by interactions between their components. Some complex systems and processes can show a behavior that is affected by the characteristics of a medium where the processes evolve. The classical models of such processes that are formulated with the linear ordinary or partial differential

equations or integrodifferential equations often do not provide a good enough description of this kind of dynamics. Therefore, fractional order operators have been used to sufficiently describe such processes [4]. FC is applied in an increasing number of fields, namely, in the area of electromagnetism [5], control engineering and signal processing [6], viscoelasticity [7], electrochemistry [8], biological population model [9], and optics [10]. The discipline of mathematical psychology, where fractional order systems could be applied to model human behavior, is an entirely separate and quite unique application field. To put it another way, humans have memories, and fractional operators are an excellent tool for modeling memory-related phenomena. Besides this, the fractional differential equation can help us to reduce the errors arising from the neglected parameters in molding real life phenomena.

Due to a wide range of applications equation with differential and integral operators, fractional orders have been studied extensively by the research community. For example, in [11], the authors have studied the analytic solutions of fractional order differential equations (FODEs) using the homotopy analysis method. Gill et al. [12] obtained the analytic solution of FODE associated with RLC circuit using Sumudu transform. In [13], the authors studied the analytic solutions of FODEs using the homotopy analysis method. Ismail et al. [14] utilized the natural transform method for the analytic solutions of FODE of the oscillator in a resisting medium. Senol [15] has utilized the new extended direct algebraic method for the new exact wave solutions of the symmetric regularized-long-wave equation with the conformable fractional derivative. Malesza et al. [16] studied the analytical solution of FODEs. In [17], the authors have implemented the invariant subspace method for obtaining the solutions of FODEs. Other efficient work on the solution of FODEs can be found in [18–22] and references therein.

A large number of valuable works on the existence and uniqueness results for the solutions of FODEs are available. For example, in [23], the authors have discussed the existence and uniqueness of the solutions of FODEs. Liu et al. [24] have studied the existence and uniqueness of FODE with nonlinear boundary conditions. In [25], the author has studied the existence of solutions of ordinary and delay FODEs. The authors of [26] studied the existence and uniqueness for the solutions of fractional order integrodifferential equations in the Banach space. In [27], the authors studied the existence and uniqueness for the solutions of fractional order Volterra–Fredholm

integrodifferential equations. Other valuable works on the existence and uniqueness of fractional order integrodifferential equations can be found in [28] and references therein.

However, in many situations, the analytic solution becomes hard to compute; therefore, we need to use numerical techniques for obtaining the solutions of FODEs. In the literature, a large number of numerical techniques are proposed for solving FODEs. For example, in [29], the authors have studied the numerical solution of FODEs using the generalized block pulse operational matrix. Esmaeili et al. [30] studied the numerical solutions of FODEs using a collocation method based on Müntz polynomials. Zabidi et al. [31] have proposed an Adams-type multistep method for the numerical solution of FODEs. In [32], the authors studied the numerical solution of FODEs using the Hadamard derivative and integral. In [33], the authors studied the numerical solution of fractional order Fredholm integrodifferential equations with the Atangana–Baleanu derivative. The authors of [34] studied the numerical solution of fractional order Volterra integrodifferential equations with the Atangana–Baleanu derivative using the Laplace transform and the contour integration method. Other efficient methods on the numerical study of fractional order integrodifferential equations can be found in [35] and references therein.

Recently, a new concept of differentiation and integration was suggested where the operator has two orders; the first is the fractional order and the second is fractal dimension such the operator is called the fractal-fractional operator [36]. This new concept can be used in many situations to solve complex problems. This concept of fractal-fractional derivative is better than the classical one and fractional derivatives as well. It is because working with fractal-fractional derivatives allows us to explore both the fractional operator and fractal dimension at the same time. Fractal-fractional differential equations are very important topics nowadays. Some important works on the study of differential and integrodifferential equations involving fractal-fractional operators can be found in [37–42]. In this work, a new class of integrodifferential equations with the Caputo fractal-fractional derivative operator is introduced. The exact solutions of these equations are derived using the method proposed in [37]. We also investigate the proposed integrodifferential equations numerically and compare the exact solutions with the numerical solutions. We consider integrodifferential equations with the fractal-fractional derivative of the following form:

$${}_{0}^{\text{FFP}} D_{\tau}^{\sigma, \varsigma} \mathcal{Y}(\tau) + \int_0^{\tau} g(\tau - \nu) \mathcal{Y}(\nu) d\tau = h(\tau), \text{ for } \tau > 0, \mathcal{Y}(0) = \mathcal{Y}_0, \quad 0 < \sigma, \varsigma \leq 1. \quad (1)$$

Integrodifferential equations have been studied very well under the usual derivative or famous Caputo's fractional order operators, but the aforementioned problems have not

been considered under the concept of fractal-fractional differential operators since fractal-fractional differential operators describe the complex and irregular shaped

geometry of phenomenon more brilliantly. Therefore, it is needed to investigate a class of integrodifferential equations under the fractal-fractional concept. Also, we need to develop some updated techniques to compute their analytical or numerical solution.

The rest of the paper is organized as follows: in Section 1.1, some basic definitions from fractional calculus are given. In Section 2, the methodology of the proposed numerical scheme is described. In Section 3, the numerical examples are given. In Section 4, some conclusions are drawn.

1.1. Preliminaries. Some basic definitions which will help us to solve fractal-fractional integrodifferential equations are as follow.

Definition 1. The Riemann–Liouville (RL) fractional derivative of the fractional order $0 < \sigma \leq 1$ is defined as follows [37]:

$${}_{0}^{RL} D_{\tau}^{\sigma} \mathcal{Y}(\tau) = \frac{1}{\Gamma(1-\sigma)} \frac{d}{d\tau} \int_0^{\tau} \mathcal{Y}(\mu) (\tau - \mu)^{-\sigma} d\mu. \quad (2)$$

Definition 2. The Caputo's derivative of the fractional order $0 < \sigma \leq 1$ is defined as follows [37]:

$${}_{0}^C D_{\tau}^{\sigma} \mathcal{Y}(\tau) = \frac{1}{\Gamma(1-\sigma)} \int_0^{\tau} \frac{d\mathcal{Y}(\mu)}{d\mu} (\tau - \mu)^{-\sigma} d\mu. \quad (3)$$

Definition 3. Let $\mathcal{Y}(\tau)$ be a continuous function on (a, b) , if $\mathcal{Y}(\tau)$ is fractal differentiable function on (a, b) with order ζ , then the fractal-fractional derivative of $\mathcal{Y}(\tau)$ of order σ with power kernel in RL sense is given as follows [37]:

$${}_{a}^{FFP} D_{\tau}^{\sigma, \zeta} \mathcal{Y}(\tau) = \frac{1}{\Gamma(1-\sigma)} \frac{d}{d\tau^{\zeta}} \int_a^{\tau} \mathcal{Y}(\mu) (\tau - \mu)^{-\sigma} d\mu, \quad (4)$$

$$0 < \sigma, \zeta \leq 1,$$

where

$$\frac{d\mathcal{Y}(\mu)}{d\mu^{\zeta}} = \lim_{t \rightarrow \mu} \frac{\mathcal{Y}(\tau) - \mathcal{Y}(\mu)}{\tau^{\zeta} - \mu^{\zeta}}. \quad (5)$$

Definition 4. A two-parameter Mittag–Leffler (ML) function is defined as follows [43]:

$$E_{\alpha, \mu}(\tau) = \sum_{k=0}^{\infty} \frac{\tau^k}{\Gamma(k\alpha + \mu)}. \quad (6)$$

Definition 5. The Laplace transform of a function $\mathcal{Y}(\tau)$, $\tau \geq 0$ is denoted by $\mathcal{L}\{\mathcal{Y}(\tau)\}$ or $\widehat{\mathcal{Y}}(s)$ and is defined as follows [37]:

$$\mathcal{L}\{\mathcal{Y}(\tau)\} = \widehat{\mathcal{Y}}(s) = \int_0^{\infty} e^{-s\tau} \mathcal{Y}(\tau) d\tau. \quad (7)$$

The Laplace transform of the ML function is given by [37]

$$\mathcal{L}\{\tau^{\mu-1} E_{\alpha, \mu}(-\delta\tau^{\alpha})\} = \frac{s^{-\alpha-\mu}}{s^{\alpha} + \delta}. \quad (8)$$

The Laplace transform of Caputo's derivative ${}_{0}^C D_{t}^{\alpha} \mathcal{Y}(\tau)$ is defined as follows [37]:

$$\mathcal{L}\left\{{}_{0}^C D_{t}^{\sigma} \mathcal{Y}(\tau)\right\} = s^{\sigma} \widehat{\mathcal{Y}}(s) - s^{\sigma-1} \mathcal{Y}(0). \quad (9)$$

For the existence and uniqueness of the solution of the fractal-fractional integrodifferential equation defined in equation (1), the following theorem will be needed.

Theorem 6 (see [38]). *If g and h are continuous in $0 < \tau < \infty$ and $-\infty < \mathcal{Y}(\tau) < \infty$ and if in addition, g and h are Lipschitz, then equation (1) has a solution.*

2. Methodology

In this section, we describe the method for obtaining the solution of fractal-fractional integrodifferential equations. Let us consider a linear fractal-fractional integrodifferential equation with a power law kernel as follows:

$${}_{0}^{FFP} D_{\tau}^{\sigma, \zeta} \mathcal{Y}(\tau) + \int_0^{\tau} g(\tau - \nu) \mathcal{Y}(\nu) d\nu = h(\tau), \quad (10)$$

$$= h(\tau), \text{ for } \tau > 0, \mathcal{Y}(0) = \mathcal{Y}_0, 0 < \sigma, \zeta \leq 1,$$

and using the definition of the RL fractal-fractional derivative, we have

$$\frac{1}{\Gamma(1-\sigma)} \frac{d}{d\tau^{\zeta}} \int_0^{\tau} \mathcal{Y}(\mu) (\tau - \mu)^{-\sigma} d\mu + \int_0^{\tau} g(\tau - \nu) \mathcal{Y}(\nu) d\nu = h(\tau), \quad (11)$$

$$\frac{1}{\Gamma(1-\sigma)} \frac{1}{\zeta \tau^{\zeta-1}} \frac{d}{d\tau} \int_0^{\tau} \mathcal{Y}(\mu) (\tau - \mu)^{-\sigma} d\mu + \int_0^{\tau} g(\tau - \nu) \mathcal{Y}(\nu) d\nu = h(\tau), \quad (12)$$

$$\frac{1}{\Gamma(1-\sigma)} \frac{d}{d\tau} \int_0^\tau \mathcal{Y}(\mu) (\tau-\mu)^{-\sigma} d\mu = \zeta \tau^{\zeta-1} h(\tau) - \zeta \tau^{\zeta-1} \int_0^\tau g(\tau-\nu) \mathcal{Y}(\nu) d\nu, \quad (13)$$

then we have

$${}_{0}^{RL} D_{\tau}^{\sigma} \mathcal{Y}(\tau) = \zeta \tau^{\zeta-1} h(\tau) - \zeta \tau^{\zeta-1} \int_0^\tau g(\tau-\nu) \mathcal{Y}(\nu) d\nu, \quad (14)$$

and using the relation between RL and Caputo's derivative, we get

$${}_{0}^c D_{\tau}^{\sigma} \mathcal{Y}(\tau) = \zeta \tau^{\zeta-1} h(\tau) - \zeta \tau^{\zeta-1} \int_0^\tau g(\tau-\nu) \mathcal{Y}(\nu) d\nu - \frac{\mathcal{Y}_0}{\Gamma(1-\sigma)} \tau^{-\sigma}. \quad (15)$$

Now, applying the Laplace transform on both sides, we have

$$s^{\sigma} \widehat{\mathcal{Y}}(s) - s^{\sigma-1} \mathcal{Y}_0 = \widehat{H}(s) - \frac{\mathcal{Y}_0 s^{\sigma-1} \Gamma(1-\sigma)}{\Gamma(1-\sigma)}, \quad (16)$$

where

$$\widehat{H}(s) = \mathcal{L} \left\{ \zeta \tau^{\zeta-1} h(\tau) - \zeta \tau^{\zeta-1} \int_0^\tau g(\tau-\nu) \mathcal{Y}(\nu) d\nu \right\}. \quad (17)$$

Simplifying (16), we get

$$\widehat{\mathcal{Y}}(s) = \frac{\widehat{H}(s)}{s^{\sigma}}, \quad (18)$$

and taking the inverse Laplace transform of (18) will give us our desired solution $\mathcal{Y}(\tau)$ as follows:

$$\mathcal{Y}(\tau) = \frac{1}{2\pi i} \int_{\rho-i\infty}^{\rho+i\infty} e^{s\tau} \widehat{\mathcal{Y}}(s) ds \quad (19)$$

$$= \frac{1}{2\pi i} \int_{\Gamma} e^{s\tau} \widehat{\mathcal{Y}}(s) ds, \text{ Real}(\rho) > \rho_0.$$

In this article, our aim is to evaluate the integral defined in equation (19), and for this purpose, we propose two types of approaches: (i) the analytic approach and (ii) the numerical approach.

2.1. Analytic Inversion of the Laplace Transform. In this section, we investigate the solutions of different fractal-fractional integrodifferential equations of the fractional order σ in RL sense with power law kernel using the method proposed in [37]. We investigate our method for three different problems of the fractal-fractional order.

2.1.1. Problem 1

$${}_{0}^{FFP} D_{\tau}^{\sigma, \zeta} \mathcal{Y}(\tau) = \tau - \tau^{1-\zeta} \int_0^\tau (\tau-\nu) \mathcal{Y}(\nu) d\nu. \quad (20)$$

Using the definition of the RL fractal-fractional derivative, we have

$$\frac{1}{\Gamma(1-\sigma)} \frac{d}{d\tau^{\zeta}} \int_0^\tau \mathcal{Y}(\mu) (\tau-\mu)^{-\sigma} d\mu = \tau - \tau^{1-\zeta} \int_0^\tau \mathcal{Y}(\nu) (\tau-\nu) d\nu, \quad (21)$$

$$\frac{1}{\Gamma(1-\sigma)} \frac{1}{\zeta \tau^{\zeta-1}} \frac{d}{d\tau} \int_0^\tau \mathcal{Y}(\mu) (\tau-\mu)^{-\sigma} d\mu = \tau - \tau^{1-\zeta} \int_0^\tau \mathcal{Y}(\nu) (\tau-\nu) d\nu, \quad (22)$$

$$\frac{1}{\Gamma(1-\sigma)} \frac{d}{d\tau} \int_0^\tau \mathcal{Y}(\mu) (\tau-\mu)^{-\sigma} d\mu = \zeta \tau^{\zeta-1} \left[\tau - \tau^{1-\zeta} \int_0^\tau \mathcal{Y}(\nu) (\tau-\nu) d\nu \right], \quad (23)$$

$${}_{0}^{RL} D_{\tau}^{\sigma} \mathcal{Y}(\tau) = \zeta \tau^{\zeta} - \zeta \int_0^\tau \mathcal{Y}(\nu) (\tau-\nu) d\nu, \quad (24)$$

and using the relation between RL and Caputo's derivative, we get

$${}_0^c D_\tau^\sigma \mathcal{Y}(\tau) = \zeta \tau^\zeta - \zeta \int_0^\tau \mathcal{Y}(\nu) (\tau - \nu) d\nu - \frac{\mathcal{Y}(0)}{\Gamma(1-\sigma)} \tau^{-\sigma}. \quad (25)$$

Taking the Laplace transform on both sides of equation (25), we get

$$s^\sigma \widehat{\mathcal{Y}}(s) - \mathcal{Y}(0) s^{\sigma-1} = \zeta \frac{\Gamma(1+\zeta)}{s^{\zeta+1}} - \zeta \frac{\widehat{\mathcal{Y}}(s)}{s^2} - \frac{\mathcal{Y}(0) s^{\sigma-1} \Gamma(1-\sigma)}{\Gamma(1-\sigma)}, \quad (26)$$

$$s^\sigma \widehat{\mathcal{Y}}(s) = s^{-\zeta-1} \zeta \Gamma(1+\zeta) - \zeta \frac{\widehat{\mathcal{Y}}(s)}{s^2}, \quad (27)$$

$$\widehat{\mathcal{Y}}(s) = \zeta \Gamma(1+\zeta) \left[\frac{s^{-\zeta+1}}{s^{\sigma+2} + \zeta} \right], \quad (28)$$

and taking the inverse Laplace transform, we obtain the exact solution as follows:

$$\mathcal{Y}(\tau) = \zeta \Gamma(1+\zeta) \tau^{\sigma+\zeta} E_{\sigma+2, \sigma+\zeta+1}(-\zeta \tau^{\sigma+2}). \quad (29)$$

$${}_0^{\text{FFP}} D_\tau^{\sigma, \zeta} \mathcal{Y}(\tau) = \tau^2 - \tau^{1-\zeta} \int_0^\tau (\tau - \nu)^2 \mathcal{Y}(\nu) d\nu. \quad (30)$$

Using the definition of RL fractal-fractional derivative, we have

2.1.2. Problem 2

$$\frac{1}{\Gamma(1-\sigma)} \frac{d}{d\tau^\zeta} \int_0^\tau \mathcal{Y}(\mu) (\tau - \mu)^{-\sigma} d\mu = \tau^2 - \tau^{1-\zeta} \int_0^\tau (\tau - \nu)^2 \mathcal{Y}(\nu) d\nu, \quad (31)$$

$$\frac{1}{\Gamma(1-\sigma)} \frac{1}{\zeta \tau^{\zeta-1}} \frac{d}{d\tau} \int_0^\tau \mathcal{Y}(\mu) (\tau - \mu)^{-\sigma} d\mu = \tau^2 - \tau^{1-\zeta} \int_0^\tau (\tau - \nu)^2 \mathcal{Y}(\nu) d\nu, \quad (32)$$

$$\frac{1}{\Gamma(1-\sigma)} \frac{d}{d\tau} \int_0^\tau \mathcal{Y}(\mu) (\tau - \mu)^{-\sigma} d\mu = \zeta \tau^{\zeta-1} \left[\tau^2 - \tau^{1-\zeta} \int_0^\tau (\tau - \nu)^2 \mathcal{Y}(\nu) d\nu \right], \quad (33)$$

$${}^{\text{RL}} D_\tau^\sigma \mathcal{Y}(\tau) = \zeta \tau^{\zeta+1} - \zeta \int_0^\tau (\tau - \nu)^2 \mathcal{Y}(\nu) d\nu, \quad (34)$$

and using the relation between RL and Caputo's derivative, we get

$${}_0^c D_\tau^\sigma \mathcal{Y}(\tau) = \zeta \tau^\zeta - \zeta \int_0^\tau \mathcal{Y}(\mu)(\tau - \nu) d\nu - \frac{\mathcal{Y}(0)}{\Gamma(1-\sigma)} \tau^{-\sigma}. \quad (35)$$

Taking the Laplace transform on both sides of equation (45), we get

$$s^\sigma \widehat{\mathcal{Y}}(s) - \mathcal{Y}(0)s^{\sigma-1} = \zeta \frac{\Gamma(2+\zeta)}{s^{\zeta+2}} - 2\zeta \frac{\widehat{\mathcal{Y}}(s)}{s^3} - \frac{\mathcal{Y}(0)s^{\sigma-1}\Gamma(1-\sigma)}{\Gamma(1-\sigma)}, \quad (36)$$

$$s^\sigma \widehat{\mathcal{Y}}(s) = s^{-\zeta-2} \zeta \Gamma(2+\zeta) - 2\zeta \frac{\widehat{\mathcal{Y}}(s)}{s^3}, \quad (37)$$

$$\widehat{\mathcal{Y}}(s) = \zeta \Gamma(2+\zeta) \left[\frac{s^{-\zeta+1}}{s^{\sigma+3} + 2\zeta} \right]. \quad (38)$$

Taking the inverse Laplace transform, we get the exact solution as follows:

$$\mathcal{Y}(\tau) = \zeta \Gamma(2+\zeta) \tau^{\sigma+\zeta+1} E_{\sigma+3, \sigma+\zeta+2}(-2\zeta \tau^{\sigma+3}). \quad (39)$$

$${}_{0^+}^{\text{FFP}} D_\tau^{\sigma, \zeta} \mathcal{Y}(\tau) = \tau^3 - \tau^{1-\zeta} \int_0^\tau (\tau - \nu)^3 \mathcal{Y}(\nu) d\nu. \quad (40)$$

Using the definition of RL fractal-fractional derivative, we have

2.1.3. Problem 3.

$$\frac{1}{\Gamma(1-\sigma)} \frac{d}{d\tau^\zeta} \int_0^\tau \mathcal{Y}(\mu)(\tau - \mu)^{-\sigma} d\mu = \tau^3 - \tau^{1-\zeta} \int_0^\tau (\tau - \nu)^3 \mathcal{Y}(\nu) d\nu, \quad (41)$$

$$\frac{1}{\Gamma(1-\sigma)} \frac{1}{\zeta \tau^{\zeta-1}} \frac{d}{d\tau} \int_0^\tau \mathcal{Y}(\mu)(\tau - \mu)^{-\sigma} d\mu = \tau^3 - \tau^{1-\zeta} \int_0^\tau (\tau - \nu)^3 \mathcal{Y}(\nu) d\nu, \quad (42)$$

$$\frac{1}{\Gamma(1-\sigma)} \frac{d}{d\tau} \int_0^\tau \mathcal{Y}(\mu)(\tau - \mu)^{-\sigma} d\mu = \zeta \tau^{\zeta-1} \left[\tau^3 - \tau^{1-\zeta} \int_0^\tau (\tau - \nu)^3 \mathcal{Y}(\nu) d\nu \right], \quad (43)$$

$${}_{0^+}^{\text{RL}} D_\tau^\sigma \mathcal{Y}(\tau) = \zeta \tau^{\zeta+2} - \zeta \int_0^\tau (\tau - \nu)^3 \mathcal{Y}(\nu) d\nu, \quad (44)$$

and using the relation between RL and Caputo's derivative, we get

$${}_{0^+}^c D_\tau^\sigma \mathcal{Y}(\tau) = \zeta \tau^{\zeta+2} - \zeta \int_0^\tau (\tau - \nu)^3 \mathcal{Y}(\nu) d\nu - \frac{\mathcal{Y}(0)}{\Gamma(1-\sigma)} \tau^{-\sigma}. \quad (45)$$

Taking the Laplace transform on both sides of equation (45), we get

$$s^\sigma \widehat{\mathcal{Y}}(s) - \mathcal{Y}(0)s^{\sigma-1} = \zeta \frac{\Gamma(3+\zeta)}{s^{\zeta+3}} - 6\zeta \frac{\widehat{\mathcal{Y}}(s)}{s^4} - \frac{\mathcal{Y}(0)s^{\sigma-1}\Gamma(1-\sigma)}{\Gamma(1-\sigma)}, \quad (46)$$

$$s^\sigma \widehat{\mathcal{Y}}(s) = \zeta s^{-\zeta-3} \Gamma(1+\zeta) - 6\zeta \frac{\widehat{\mathcal{Y}}(s)}{s^4}, \quad (47)$$

$$\widehat{\mathcal{Y}}(s) = \zeta\Gamma(3 + \zeta) \left[\frac{s^{-\zeta+1}}{s^{\sigma+4} + 6\zeta} \right]. \quad (48)$$

Taking the inverse Laplace transform, we get the exact solution as follows:

$$\mathcal{Y}(\tau) = \zeta\Gamma(3 + \zeta)\tau^{\sigma+\zeta+2} E_{\sigma+4, \sigma+\zeta+3}(-6\zeta\tau^{\sigma+4}). \quad (49)$$

2.2. Numerical Inversion of the Laplace Transform. In many situations, when the function $\widehat{\mathcal{Y}}(s)$ is complicated, the Bromwich integral defined in equation (19) cannot be evaluated easily. For instance, when the transform $\widehat{\mathcal{Y}}(s)$ is a highly oscillatory function, then the closed form solution of equation (19) is generally not available. Therefore, we need to use numerical methods for the approximation of the Bromwich integral defined in equation (19). In this section, we study five different numerical inverse Laplace transform (NILT) methods for this purpose.

2.2.1. Contour Integration Method. Various methods for the numerical inversion of the Laplace transform are based on the quadrature approximation of the integral defined in (19). In these methods, it is assumed that the transform function $\widehat{\mathcal{Y}}(s)$ is analytic in the complex plane $\text{Re}(s) > \rho_0$ with ρ_0 the converging abscissa, where the contour Γ is a line $\text{Re}(s) = \rho$ with $\rho > \rho_0$. However, the deformation of the line $\text{Re}(s) = \rho$ to a contour of integration is possible via Cauchy's theorem. Such deformation methods are useful for the analytic and numerical solution of (19). For numerical solution, we proceed as follows: on the line $\text{Re}(s) = \rho$, the integral defined in (19) is not ideally suitable by quadrature because of the oscillatory nature of $\exp(s\tau)$ and the slow decay of the transform $|\widehat{\mathcal{Y}}(s)|$ as $\text{Im}(s) \rightarrow \infty$. By deforming the Bromwich line $\text{Re}(s) = \rho$ into a contour which starts at infinity in the 3rd quadrant and winds around all singularities of the transform $\widehat{\mathcal{Y}}(s)$ and ends in 2nd quadrant, the slow decay of the transform $\widehat{\mathcal{Y}}(s)$ can be exploited. This contour deformation is valid if the contour encloses all the singularities of the transform $\widehat{\mathcal{Y}}(s)$ and $|\widehat{\mathcal{Y}}(s)| \rightarrow 0$ uniformly as $\text{Re}(s) \leq \rho_0$ and $s \rightarrow \infty$ [44]. For the workable numerical strategy and optimal results, the numerical scheme relies upon two factors: (i) the choice of contour of integration and (ii) the choice of the quadrature rule. In the literature, the researchers have focused mainly on the contours as well as the optimal parameters for each such contour [45, 46]. In this paper, we consider the improved version of Talbot's contour proposed in [47] and the hyperbolic contour proposed in [46].

(1) *Talbot's Contour (TLM).* Here, we consider a contour of the following form [47]:

$$\Gamma: s = s(\eta), -\pi \leq \eta \leq \pi, \quad (50)$$

$\text{Res}(\pm \pi) = -\text{inf}$, and $s(\eta)$ is given as follows:

$$s(\eta) = \frac{M_T}{\tau} \zeta(\eta), \zeta(\eta) = -\delta + \sigma\eta \cot(\mu\eta) + \gamma i\eta, \quad (51)$$

where μ, ν , and γ are to be chosen by the user. Using equations (51) in (19), we get

$$\mathcal{Y}(\tau) = \frac{1}{2\pi i} \int_{-\pi}^{\pi} e^{s(\eta)\tau} \widehat{\mathcal{Y}}(s) (s(\eta))' s'(\eta) d\eta. \quad (52)$$

The integral defined in (52) is approximated via midpoint rule with spacing $h = 2\pi/M_T$ as follows:

$$\begin{aligned} \mathcal{Y}_{\text{App}}(\tau) &\approx \frac{1}{M_T i} \sum_{k=1}^{M_T} e^{s(\eta_k)\tau} \widehat{\mathcal{Y}}(s(\eta_k)) s'(\eta_k), \eta_k \\ &= -\pi + \left(k - \frac{1}{2}\right)h. \end{aligned} \quad (53)$$

(2) *Convergence.* In the approximation of the integral defined in equation (52), the convergence of the proposed numerical scheme is achieved at different rates depending on the contour of integration Γ . Also, the convergence of the proposed scheme depends on the quadrature step h . In order to have optimal results, we need to search for the optimal contour of integration, which can be done by using the optimal values of the parameters involved in (51). The authors in [47] have proposed optimal values of the parameters as follows:

$$\begin{aligned} \delta &= 0.61220, \\ \gamma &= 0.26450, \\ \mu &= 0.6407, \text{ and} \\ \sigma &= 0.5017. \end{aligned} \quad (54)$$

The error estimate of the improved Talbot's method is given as follows:

$$\text{Error}_{\text{est}} = \left| \mathcal{Y}_{\text{App}}(\tau) - \mathcal{Y}(\tau) \right| = O\left(e^{-1.35800M_T}\right). \quad (55)$$

(3) *Hyperbolic Contour (HYM).* We also use the hyperbolic contour proposed in [46] which is defined as

$$s(\eta) = \omega + \lambda(1 - \sin(\delta - i\eta)), \text{ for } \eta \in \mathbb{R}, \quad (56)$$

with $\lambda > 0$, $\omega \geq 0$, $0 < \delta < \zeta - 1/2\pi$, and $1/2\pi < \zeta < \pi$ (for detail see [46]). Using equation (56) in equation (19), we get

$$\mathcal{Y}(\tau) = \frac{1}{2\pi i} \int_{\Gamma} e^{s\tau} \widehat{\mathcal{Y}}(s) ds = \frac{1}{2\pi i} \int_{-\infty}^{\infty} e^{s(\eta)\tau} \widehat{\mathcal{Y}}(s(\eta)) s'(\eta) d\eta. \quad (57)$$

The integral defined (52) can be approximated via the trapezoidal rule with step k as follows:

$$\mathcal{Y}_{\text{App}}(\tau) = \frac{k}{2\pi i} \sum_{j=-M_H}^{M_H} e^{s_j \tau} \widehat{\mathcal{Y}}(s_j) s'_j, s_j = s(\eta_j), \eta_j = jk. \quad (58)$$

(4) *Convergence.* Here, we discuss the convergence of the proposed numerical inverse Laplace transform method. While approximating the integral defined in (57), we achieve the convergence at different time rates which depends on the contour of integration Γ . The convergence order of the proposed numerical method depends on the step k of the quadrature rule and the temporal $[t_0, T]$. The proof for the convergence order for the contour Γ is given in the following theorem.

Theorem 7 (see [46], Theorem 8). *Let $\mathcal{Y}(\tau)$ be the solution of (8) with $\widehat{H}(s) = \mathcal{L}\{h(t)\}$ be the analytic function in the set Σ_{φ}^Y . Let $\Gamma \subset \Omega_r \subset \Sigma_{\varphi}^Y$, and define the constant $b > 0$ by the relation $b = \cos h^{-1}\{1/\theta\tau_1 \sin(\eta)\}$, where $\tau_1 = t_0/T$, $0 < \theta < 1$, $0 < \tau_0 < T$; also, let $\bar{\omega} = \theta\bar{r}M/bT$. Then, for $\mathcal{Y}_{\text{App}}(\tau)$ defined in equation (53), we have $|\mathcal{Y}(\tau) - \mathcal{Y}_{\text{App}}(\tau)| \leq CQe^{Y\tau_1} l(\rho_r M)e^{-\bar{\omega}M} (\|\mathcal{Y}_0\| + \|\widehat{H}(s)\|_{\Sigma_{\varphi}^Y})$, with $\bar{\omega} = \bar{r}(1 - \theta)/b$, $k = b/M_H \leq \bar{r}/\log 2$, $\rho_r = \theta\bar{r}\tau_1 \sin(\eta - r_1)/b$, $\bar{r} = 2\pi r_1$, $r_1 > 0$, $\tau_0 \leq \tau \leq T$, $C = C_{\eta, r_1, \varphi}$ and $l(x) = \max(1, \log(1/x))$. Hence, the error estimate is given as follows:*

$$\text{error}_{\text{est}} = |\mathcal{Y}(\tau) - \mathcal{Y}_{\text{App}}(\tau)| = O(l(\rho_r M)e^{-\bar{\omega}M_H}). \quad (59)$$

2.2.2. *Stehfest Method (STM).* The Gaver–Stehfest algorithm is one of the most important algorithms used for the numerical inversion of the Laplace transform. It was developed in the late 1960s. Due to its simplicity and performance, it is becoming popular in many areas such as economics, geophysics, financial mathematics, chemistry, and computational physics. The Gaver–Stehfest algorithm is based on the

sequence of Gaver approximants, derived by Gaver [48]. Since the convergence of the Gaver approximants was only logarithmic, it needed acceleration. A linear acceleration method was proposed by Stehfest [49], using the Salzer acceleration scheme. Gaver–Stehfest’s method approximate $\mathcal{Y}(\tau)$ by a sequence of functions given as follows:

$$\mathcal{Y}_{\text{App}}(\tau) = \frac{\ln 2}{\tau} \sum_{i=1}^{2M_S} W_i \widehat{\mathcal{Y}}\left(\frac{\ln 2}{\tau} i\right), \quad (60)$$

where the coefficients W_i are defined by

$$W_i = (-1)^{M_S+i} \sum_{l=[i+1/2]}^{\min(i, M_S)} \frac{l^{M_S} (2l)!}{(M_S - l)!! (l - 1)! (i - l)! (2l - i)!}. \quad (61)$$

Solving (15) for the corresponding Laplace parameters $s = \ln 2/\tau i$, $i = 1, 2, 3, \dots, M_S$, the solution of the original problem can be obtained using (54). The Gaver–Stehfest algorithm has some attractive properties: (i) the approximations $\mathcal{Y}_{\text{App}}(\tau)$ are linear in values of $\widehat{\mathcal{Y}}(s)$; (ii) it requires the values of $\widehat{\mathcal{Y}}(s)$ for real s only; (iii) the computation of the coefficients is very easy; and (iv) the approximations using this algorithm are exact for constant functions, that is, if $\mathcal{Y}(\tau) \equiv c$, then $\mathcal{Y}_{\text{App}}(\tau) \equiv c$ for all $M_S \geq 1$. In the literature, this algorithm has been studied by many authors in [50, 51], where it is demonstrated that this method converges very fast to $\mathcal{Y}(\tau)$ (provided $\mathcal{Y}(\tau)$ is nonoscillatory).

(1) *Convergence of the STM.* Kuznetsov in [50] has derived two sufficient conditions on the function $\mathcal{Y}(\tau)$, which ensures the convergence of $\mathcal{Y}_{\text{App}}(\tau)$. The results are mainly based on the following theorem.

Theorem 8. *Assume $\mathcal{Y}: (0, \infty) \rightarrow \mathbb{R}$ is a locally integrable function such that its Laplace transform $\widehat{\mathcal{Y}}(s)$ exists for all $s > 0$ and that $\mathcal{Y}_{\text{App}}(\tau)$ are defined by (54) the following.*

- (1) *The convergence of $\mathcal{Y}_{\text{App}}(\tau)$ depends only on the values of $\mathcal{Y}(\tau)$ in the neighborhood of τ .*
- (2) *Assume that for some $m \in \mathbb{R}$ and some $\varepsilon \in (0, 1/4)$, then we have*

$$\int_0^{\varepsilon} |\mathcal{Y}(-x \log_2(1/2 + \nu)) + \mathcal{Y}(-x \log_2(1/2 - \nu)) - 2m|\nu|^{-1} d\nu < \infty. \quad (62)$$

Then, $\mathcal{Y}_{\text{App}}(\tau) \rightarrow m$ as $M_S \rightarrow +\infty$.

- (3) *Assume that the function has bounded variation in the neighborhood of τ . Then,*

$$\mathcal{Y}_{\text{App}}(\tau) \rightarrow \frac{\mathcal{Y}(\tau + 0) + \mathcal{Y}(\tau - 0)}{2} \text{ as } M_S \rightarrow +\infty. \quad (63)$$

Corollary 9. *Under the assumptions of the abovementioned theorem, if*

$$\mathcal{Y}(\tau + \nu) - \mathcal{Y}(\tau) = O(|\nu|^{\nu}). \quad (64)$$

$\forall \nu$ and some ν in the neighborhood of τ , then $\mathcal{Y}_{\text{App}}(\tau) \rightarrow \mathcal{Y}(\tau)$, as $M_S \rightarrow +\infty$.

Also, the authors in [52, 53] performed a number of experiments to study the parameter effect on the accuracy of the numerical scheme and they concluded their findings that “for η significant digits, let $M_S = \lceil 1.1\zeta \rceil \in \mathbb{Z}^+$. Set the system precision at $\lceil 2.2M_S \rceil$ and for given M_S , calculate $W_i, 1 \leq i \leq 2M_S$, using (61). Then, for the given transform $\widehat{\mathcal{Y}}(s)$ and the argument τ , calculate the $\mathcal{Y}_{\text{App}}(\tau)$ in (60).” According to these conclusions, the error is $10^{-(\zeta+1)} \leq \widehat{\mathcal{Y}} - \mathcal{Y}/\mathcal{Y} \leq 10^{-\zeta}$, where $M_S = \lceil 1.1\zeta \rceil$ [54].

2.2.3. Zakian’s Method (ZKM). Using Zakian’s method [55], the time domain function is approximated using the infinite series of the weighted evaluations of domain functions given as follows [56]:

$$\mathcal{Y}_{\text{App}}(\tau) = \frac{2}{\tau} \sum_{i=1}^N \text{Real} \left(K_i \widehat{\mathcal{Y}} \left(\frac{\chi_i}{\tau} \right) \right), 0 < \tau < \infty. \quad (65)$$

$$\mathcal{Y}_{\text{App}}(\tau) = \frac{\exp(a\tau)}{T} \left[\frac{1}{2} \widehat{\mathcal{Y}}(a) + \sum_{k=1}^{\infty} \left\{ \text{Re} \left\{ \widehat{\mathcal{Y}} \left(a + \frac{k\pi i}{T} \right) \right\} \cos \left(\frac{k\pi i}{T} \right) - \text{Im} \left\{ \widehat{\mathcal{Y}} \left(a + \frac{k\pi i}{T} \right) \right\} \sin \left(\frac{k\pi i}{T} \right) \right\} \right], \quad (66)$$

where

$$\mathcal{Y}(\tau) = \mathcal{Y}_{\text{App}}(\tau) - E, \quad lpc \quad (67)$$

$$E = \sum_{n=1}^{\infty} \exp(-2naT) \mathcal{Y}(2nT + \tau). \quad (68)$$

2.3. Error Analysis of the FRM. In the proposed method, there are two sources of error excluding the roundoff error. We have the error term E due to the fact that Fourier coefficients are not exact, they are obtained using the transform $\mathcal{Y}(s)$. Since the series in (57) is not summed up to infinity, there is a truncation error. Using the condition $|\mathcal{Y}(\tau)| \leq Ce^{bt}$ from (58), we have [58]

$$E \leq \frac{Ce^{bt}}{e^{2T(a-b)} - 1}, 0 < t < 2T. \quad (69)$$

It means that by selecting a sufficiently larger than b , the error E can be made as small as possible. So, the relative error can be $E_R \equiv E/Ce^{bt} \leq 0.005$, which implies that we can replace (69) by

$$E \leq Ce^{bt} e^{-2T(a-b)}, 0 < t < 2T. \quad (70)$$

3. Numerical Simulations

In this section, we validate our proposed NILT methods. We consider three different integrodifferential equations with Caputo’s fractal-fractional derivative. The performance of the proposed NILT schemes is evaluated using two error measures, the absolute error Ab_{Error} and the relative error RL_{Error} defined as follows:

This method is very easy to implement and fast. There is only one free parameter N which needs to be determined. For accurate solutions, we need the optimal value of the parameter N . A large number of methods have been proposed for obtaining the optimal values for the set of constants $\{K_i, \chi_i\}$. For $N = 5$, one set is given in Table 1.

2.2.4. Fourier Series Method (FRM). The Fourier series method for numerical inversion of the Laplace transform was first used in [57]. This method is based on choosing the contour of integration in the Bromwich integral, then converting the Bromwich integral into Fourier transform, and then using the Fourier series for the approximation of the Fourier transform. This method approximate the Bromwich integral using the following equation (58):

$$Ab_{\text{Error}} = |\mathcal{Y}_{\text{App}}(\tau) - \mathcal{Y}(\tau)|, \text{ and} \quad (71)$$

$$RL_{\text{Error}} = \left| \frac{\mathcal{Y}_{\text{App}}(\tau) - \mathcal{Y}(\tau)}{\mathcal{Y}(\tau)} \right|.$$

In the first test, we consider problem 1 defined by equation (20) with the exact solution given in equation (29). The problem is solved using five NILT schemes. In Table 2, the Ab_{Error} and RL_{Error} for problem 1 obtained using the TLM are presented. Table 3 presents the Ab_{Error} and RL_{Error} obtained using the STM. Table 4 presents the Ab_{Error} and RL_{Error} obtained using HYM. In Table 5, the Ab_{Error} and RL_{Error} obtained using the ZKM and in Table 6, the Ab_{Error} and RL_{Error} obtained using the FRM are displayed. Figure 1(a) shows the plots of numerical and analytic solutions for various values of σ and ζ using the ZKM. Figure 1(b) shows the plot of Ab_{Error} and RL_{Error} for various values of σ and ζ using the ZKM. The plots of Ab_{Error} and RL_{Error} for various values of σ and ζ using the HYM are shown in Figure 2(a), and Figure 2(b) shows the plots of Ab_{Error} and RL_{Error} of the problem using TLM. In Figure 3(a), the Ab_{Error} and RL_{Error} for various values of σ and ζ using the FRM are shown. Figure 3(b) shows plot of Ab_{Error} and RL_{Error} of the STM. Similarly, in Figure 4(a), a comparison between the Ab_{Error} using the five numerical schemes is presented, and in Figure 4(b), a comparison between RL_{Error} using the five numerical schemes is presented. It is observed that the performance of the HYM is better as compared to the other four NILT schemes.

In the second test, we consider problem 2 defined by equation (30) with exact solution given in equation (39). The problem is solved using five NILT schemes. In Table 7, the Ab_{Error} and RL_{Error} for problem 2 obtained using TLM are presented. Table 8 presents the Ab_{Error} and RL_{Error} obtained

TABLE 1: Five constants for the ZKM.

i	χ_i	K_i
1	$(1.283767675e + 1) + j1.666063445$	$(-3.69020821e + 4) + j1.96990426e + 5$
2	$(1.222613209e + 1) + j5.012718792$	$(6.12770252e + 4) - j9.54086255e + 4$
3	$(1.09343031e + 1) + j8.40967312$	$-(2.89165629e + 4) + j1.81691853e + 4$
4	$8.77643472 + j1.19218539e + 1$	$(4.65536114e + 3) - j1.90152864$
5	$5.22545336 + j1.57295290e + 1$	$-(1.18741401e + 2) - j1.41303691e + 2$

TABLE 2: The errors obtained using TLM for problem 1 with various values of σ and ζ and $M_T = 24$.

τ	$(\sigma, \zeta) = (0.25, 0.25)$		$(\sigma, \zeta) = (0.55, 0.55)$		$(\sigma, \zeta) = (0.85, 0.85)$	
	Ab_{Error}	RL_{Error}	Ab_{Error}	RL_{Error}	Ab_{Error}	RL_{Error}
0.1	1.2948×10^{-14}	1.6018×10^{-13}	2.3280×10^{-14}	6.2743×10^{-13}	2.6087×10^{-13}	2.5127×10^{-11}
0.2	1.5275×10^{-13}	1.3376×10^{-12}	8.7337×10^{-13}	1.0987×10^{-11}	1.3768×10^{-12}	4.0824×10^{-11}
0.3	3.2568×10^{-13}	2.3333×10^{-12}	3.2185×10^{-12}	2.5951×10^{-11}	1.1587×10^{-11}	1.7254×10^{-10}
0.4	1.9196×10^{-13}	1.1946×10^{-12}	3.8045×10^{-12}	2.2400×10^{-11}	3.1961×10^{-11}	2.9212×10^{-10}
0.5	7.8570×10^{-13}	4.3918×10^{-12}	7.7764×10^{-12}	3.5927×10^{-11}	2.9477×10^{-11}	1.8464×10^{-10}
0.6	3.1041×10^{-12}	1.5925×10^{-11}	4.8662×10^{-11}	1.8472×10^{-10}	1.0901×10^{-10}	5.0195×10^{-10}
0.7	6.7967×10^{-12}	3.2498×10^{-11}	1.3270×10^{-10}	4.2740×10^{-10}	6.0438×10^{-10}	2.1478×10^{-09}
0.8	1.0889×10^{-11}	4.9094×10^{-11}	2.4595×10^{-10}	6.8850×10^{-10}	1.7168×10^{-09}	4.8810×10^{-09}
0.9	1.2876×10^{-11}	5.5250×10^{-11}	3.0740×10^{-10}	7.6208×10^{-10}	3.4597×10^{-09}	8.0913×10^{-09}
1.0	8.4363×10^{-12}	3.4717×10^{-11}	1.2387×10^{-10}	2.7614×10^{-10}	4.9673×10^{-09}	9.7712×10^{-09}

TABLE 3: The errors obtained using STM for problem 1 with various values of σ and ζ and $M_S = 16$.

τ	$(\sigma, \zeta) = (0.25, 0.25)$		$(\sigma, \zeta) = (0.55, 0.55)$		$(\sigma, \zeta) = (0.85, 0.85)$	
	Ab_{Error}	RL_{Error}	Ab_{Error}	RL_{Error}	Ab_{Error}	RL_{Error}
0.1	2.8802×10^{-09}	3.5631×10^{-08}	1.8483×10^{-09}	4.9814×10^{-08}	2.6309×10^{-10}	2.5342×10^{-08}
0.2	9.5344×10^{-12}	8.3492×10^{-11}	4.1874×10^{-09}	5.2678×10^{-08}	2.3137×10^{-09}	6.8605×10^{-08}
0.3	9.9933×10^{-10}	7.1595×10^{-09}	3.7240×10^{-09}	3.0027×10^{-08}	1.8680×10^{-08}	2.7817×10^{-07}
0.4	7.9652×10^{-09}	4.9571×10^{-08}	1.4912×10^{-08}	8.7796×10^{-08}	1.8166×10^{-07}	1.6604×10^{-06}
0.5	5.7166×10^{-09}	3.1954×10^{-08}	9.4457×10^{-08}	4.3640×10^{-07}	1.2393×10^{-06}	7.7632×10^{-06}
0.6	2.1708×10^{-08}	1.1137×10^{-07}	1.4603×10^{-07}	5.5430×10^{-07}	5.0017×10^{-06}	2.3031×10^{-05}
0.7	6.5225×10^{-08}	3.1187×10^{-07}	4.8173×10^{-07}	1.5516×10^{-06}	1.1797×10^{-05}	4.1923×10^{-05}
0.8	1.6283×10^{-07}	7.3411×10^{-07}	3.7168×10^{-06}	1.0405×10^{-05}	1.0451×10^{-05}	2.9715×10^{-05}
0.9	3.5016×10^{-07}	1.5025×10^{-06}	1.3147×10^{-05}	3.2592×10^{-05}	3.7719×10^{-05}	8.8214×10^{-05}
1.0	6.7197×10^{-07}	2.7653×10^{-06}	3.2586×10^{-05}	7.2642×10^{-05}	2.0558×10^{-04}	4.0440×10^{-04}

TABLE 4: The errors obtained using HYM for problem 1 with various values of σ and ζ and $M_H = 160$.

τ	$(\sigma, \zeta) = (0.25, 0.25)$		$(\sigma, \zeta) = (0.55, 0.55)$		$(\sigma, \zeta) = (0.85, 0.85)$	
	Ab_{Error}	RL_{Error}	Ab_{Error}	RL_{Error}	Ab_{Error}	RL_{Error}
0.1	1.7084×10^{-13}	2.1135×10^{-12}	1.2981×10^{-16}	3.4985×10^{-15}	1.0748×10^{-16}	1.0353×10^{-14}
0.2	2.4371×10^{-13}	2.1342×10^{-12}	4.1005×10^{-15}	5.1585×10^{-14}	5.1068×10^{-16}	1.5143×10^{-14}
0.3	4.9545×10^{-13}	3.5495×10^{-12}	1.0187×10^{-15}	8.2136×10^{-15}	1.0548×10^{-15}	1.5707×10^{-14}
0.4	3.8405×10^{-13}	2.3901×10^{-12}	2.6354×10^{-14}	1.5517×10^{-13}	2.7754×10^{-15}	2.5367×10^{-14}
0.5	3.8597×10^{-13}	2.1575×10^{-12}	5.3334×10^{-14}	2.4641×10^{-13}	5.1356×10^{-15}	3.2169×10^{-14}
0.6	1.1727×10^{-12}	6.0164×10^{-12}	2.7387×10^{-14}	1.0396×10^{-13}	8.0386×10^{-15}	3.7015×10^{-14}
0.7	8.3151×10^{-13}	3.9758×10^{-12}	1.1667×10^{-13}	3.7577×10^{-13}	1.4652×10^{-14}	5.2070×10^{-14}
0.8	7.2165×10^{-13}	3.2536×10^{-12}	2.0446×10^{-13}	5.7236×10^{-13}	2.3308×10^{-14}	6.6268×10^{-14}
0.9	3.7438×10^{-12}	1.6064×10^{-11}	4.5410×10^{-14}	1.1258×10^{-13}	2.6649×10^{-14}	6.2325×10^{-14}
1.0	5.2379×10^{-13}	2.1555×10^{-12}	4.8322×10^{-13}	1.0772×10^{-12}	5.4136×10^{-14}	1.0649×10^{-13}

using the STM. Table 9 presents the Ab_{Error} and RL_{Error} obtained using HYM. In Table 10, the Ab_{Error} and RL_{Error} obtained using the ZKM and in Table 11, the Ab_{Error} and RL_{Error} obtained using the FRM are displayed. Figure 5(a)

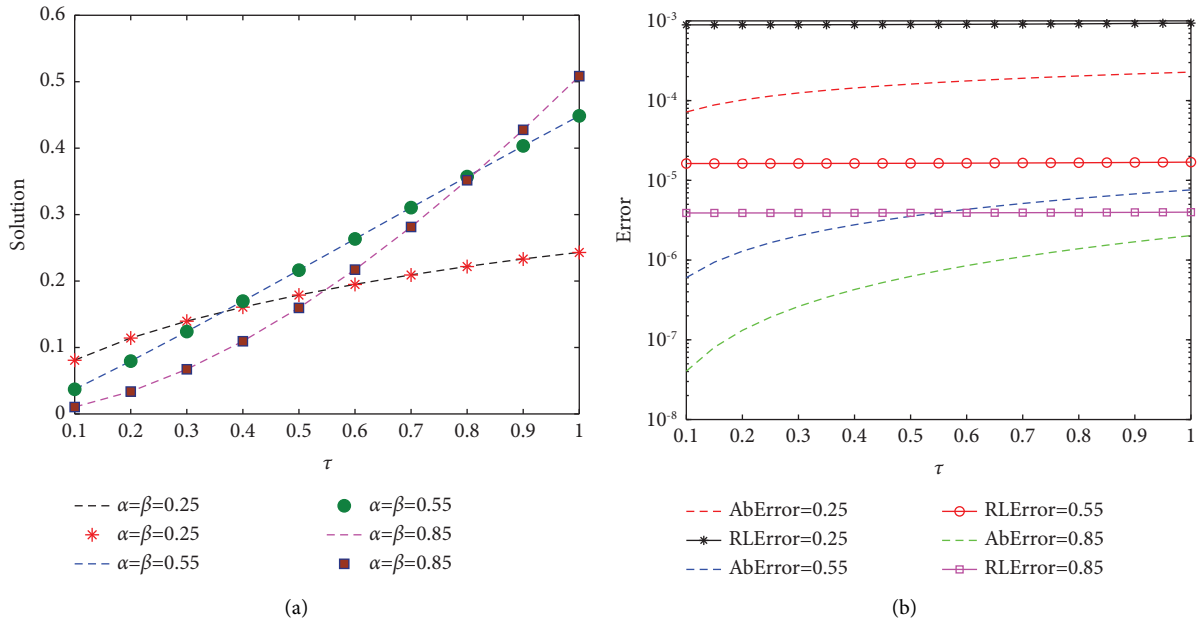
shows the plots of numerical and analytic solutions for various values of σ and ζ using the TLM. Figure 5(b) shows the plot of Ab_{Error} and RL_{Error} for various values of σ and ζ using the TLM. The plots of Ab_{Error} and RL_{Error} for various

TABLE 5: The errors obtained using the ZKM for problem 1 with various values of σ and ζ .

τ	$(\sigma, \zeta) = (0.25, 0.25)$		$(\sigma, \zeta) = (0.55, 0.55)$		$(\sigma, \zeta) = (0.85, 0.85)$	
	Ab_{Error}	RL_{Error}	Ab_{Error}	RL_{Error}	Ab_{Error}	RL_{Error}
0.1	6.8875×10^{-08}	1.0222×10^{-05}	9.8134×10^{-10}	3.5830×10^{-07}	1.1462×10^{-10}	1.6113×10^{-07}
0.2	1.9481×10^{-07}	1.0222×10^{-05}	4.2071×10^{-09}	3.5830×10^{-07}	7.4482×10^{-10}	1.6113×10^{-07}
0.3	3.5789×10^{-07}	1.0224×10^{-05}	9.8577×10^{-09}	3.5833×10^{-07}	2.2258×10^{-09}	1.6113×10^{-07}
0.4	5.5100×10^{-07}	1.0226×10^{-05}	1.8036×10^{-08}	3.5838×10^{-07}	4.8398×10^{-09}	1.6114×10^{-07}
0.5	7.7005×10^{-07}	1.0231×10^{-05}	2.8817×10^{-08}	3.5849×10^{-07}	8.8406×10^{-09}	1.6116×10^{-07}
0.6	1.0123×10^{-06}	1.0238×10^{-05}	4.2259×10^{-08}	3.5866×10^{-07}	1.4463×10^{-08}	1.6120×10^{-07}
0.7	1.2756×10^{-06}	1.0249×10^{-05}	5.8412×10^{-08}	3.5892×10^{-07}	2.1929×10^{-08}	1.6126×10^{-07}
0.8	1.5585×10^{-06}	1.0264×10^{-05}	7.7316×10^{-08}	3.5930×10^{-07}	3.1447×10^{-08}	1.6135×10^{-07}
0.9	1.8596×10^{-06}	1.0283×10^{-05}	9.9007×10^{-08}	3.5983×10^{-07}	4.3218×10^{-08}	1.6148×10^{-07}
1.0	2.1781×10^{-06}	1.0309×10^{-05}	1.2352×10^{-07}	3.6053×10^{-07}	5.7436×10^{-08}	1.6165×10^{-07}

TABLE 6: The errors obtained using the FRM for problem 1 with various values of σ and ζ and $T = 4$.

τ	$(\sigma, \zeta) = (0.25, 0.25)$		$(\sigma, \zeta) = (0.55, 0.55)$		$(\sigma, \zeta) = (0.85, 0.85)$	
	Ab_{Error}	RL_{Error}	Ab_{Error}	RL_{Error}	Ab_{Error}	RL_{Error}
0.1	1.0642×10^{-05}	1.3165×10^{-04}	4.7434×10^{-08}	1.2784×10^{-06}	5.2971×10^{-08}	5.1023×10^{-06}
0.2	6.9771×10^{-06}	6.1098×10^{-05}	2.1664×10^{-08}	2.7253×10^{-07}	6.8903×10^{-08}	2.0432×10^{-06}
0.3	6.0653×10^{-06}	4.3454×10^{-05}	1.3488×10^{-08}	1.0876×10^{-07}	8.7708×10^{-08}	1.3061×10^{-06}
0.4	5.9147×10^{-06}	3.6809×10^{-05}	8.7986×10^{-09}	5.1804×10^{-08}	1.0794×10^{-07}	9.8655×10^{-07}
0.5	6.1388×10^{-06}	3.4314×10^{-05}	4.6921×10^{-09}	2.1677×10^{-08}	1.2922×10^{-07}	8.0944×10^{-07}
0.6	6.6243×10^{-06}	3.3984×10^{-05}	4.3567×10^{-11}	1.6537×10^{-10}	1.5135×10^{-07}	6.9690×10^{-07}
0.7	7.3399×10^{-06}	3.5095×10^{-05}	6.2244×10^{-09}	2.0048×10^{-08}	1.7414×10^{-07}	6.1885×10^{-07}
0.8	8.2894×10^{-06}	3.7373×10^{-05}	1.4606×10^{-08}	4.0888×10^{-08}	1.9743×10^{-07}	5.6131×10^{-07}
0.9	9.4966×10^{-06}	4.0749×10^{-05}	2.6019×10^{-08}	6.4505×10^{-08}	2.2102×10^{-07}	5.1691×10^{-07}
1.0	1.1001×10^{-05}	4.5270×10^{-05}	4.1447×10^{-08}	9.2396×10^{-08}	2.4473×10^{-07}	4.8141×10^{-07}

FIGURE 1: (a) The comparison of the numerical solution (dashed lines) and exact solutions (markers) of problem 1 using the ZKM. (b) The comparison of Ab_{Error} (dashed lines) and RL_{Error} (markers) for problem 1 using ZKM.

values of σ and ζ using HYM are shown in Figure 6(a), and Figure 6(b) shows the plots of Ab_{Error} and RL_{Error} of the problem using the STM. In Figure 7(a), the Ab_{Error} and RL_{Error} for various values of σ and ζ using the FRM are

shown. Figure 7(b) shows plot of Ab_{Error} and RL_{Error} of the ZKM. Similarly, in Figure 8(a), a comparison between the Ab_{Error} using the five schemes is presented and in Figure 8(b) a comparison between the RL_{Error} using the five schemes is

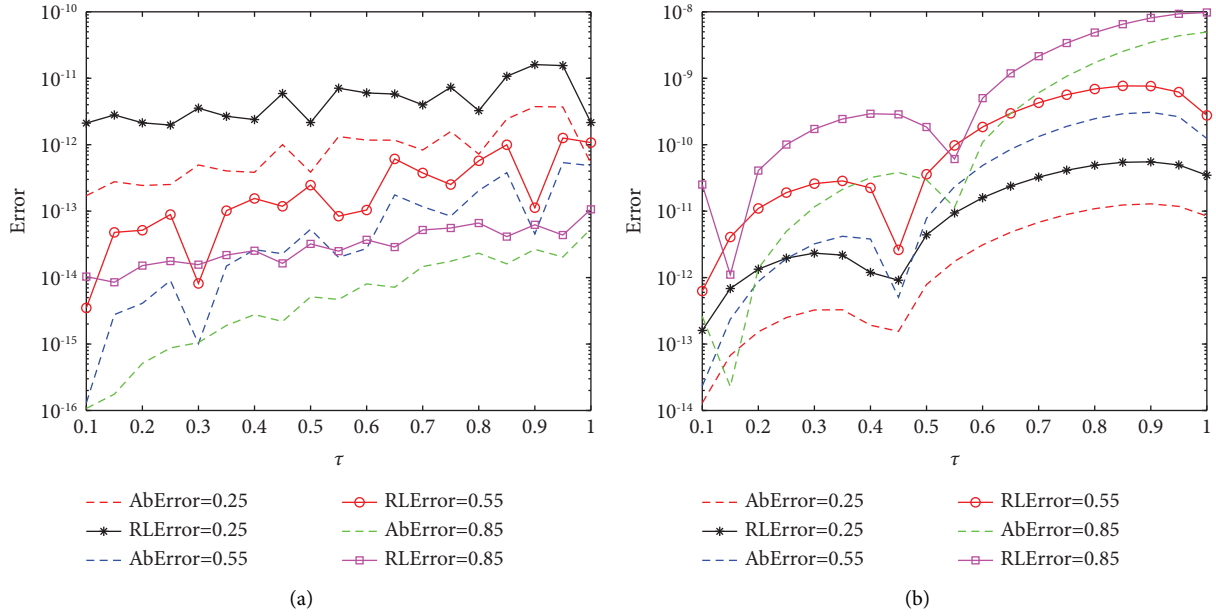


FIGURE 2: (a) The comparison of Ab_{Error} (dashed lines) and RL_{Error} (markers) for problem 1 using HYM. (b) The comparison of Ab_{Error} (dashed lines) and RL_{Error} (markers) for problem 1 using TLM.

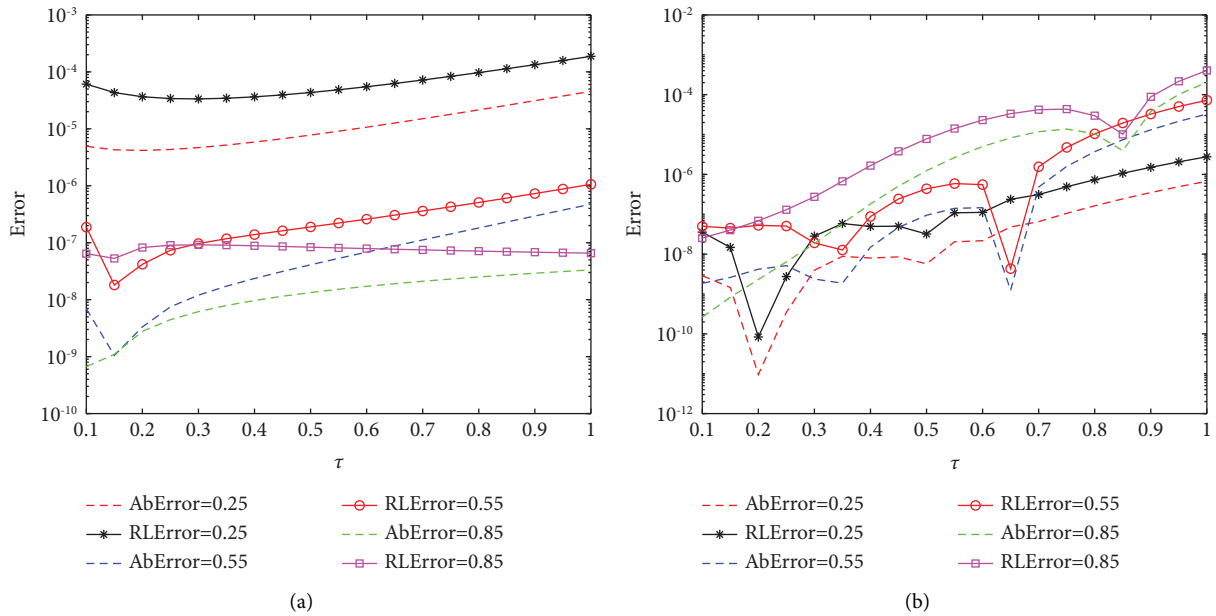


FIGURE 3: (a) The comparison of Ab_{Error} (dashed lines) and RL_{Error} (markers) for problem 1 using the FRM. (b) The comparison of Ab_{Error} (dashed lines) and RL_{Error} (markers) for problem 1 using the STM.

presented. For this problem also, all the five schemes have produced accurate results.

In the third test, we consider problem 3 defined by equation (40) with the exact solution given in equation (49). The problem is solved using five NILT schemes. In Table 12, the Ab_{Error} and RL_{Error} for problem 3 obtained using TLM are presented. Table 13 presents the Ab_{Error} and RL_{Error} obtained using the STM. Table 14 presents the Ab_{Error} and RL_{Error} obtained using HYM. In Table 15, the

Ab_{Error} and RL_{Error} obtained using the ZKM and in Table 16, the Ab_{Error} and RL_{Error} using the FRM are displayed. Figure 9(a) shows the plots of numerical and analytic solutions for various values of σ and ζ using the FRM. Figure 9(b) shows the plot of Ab_{Error} and RL_{Error} for various values of σ and ζ using the FRM. The plots of Ab_{Error} and RL_{Error} for various values of σ and ζ using the TLM are shown in Figures 10(a) and 10(b) shows the plots of Ab_{Error} and RL_{Error} of problem 3 using HYM. In Figure 11(a), the

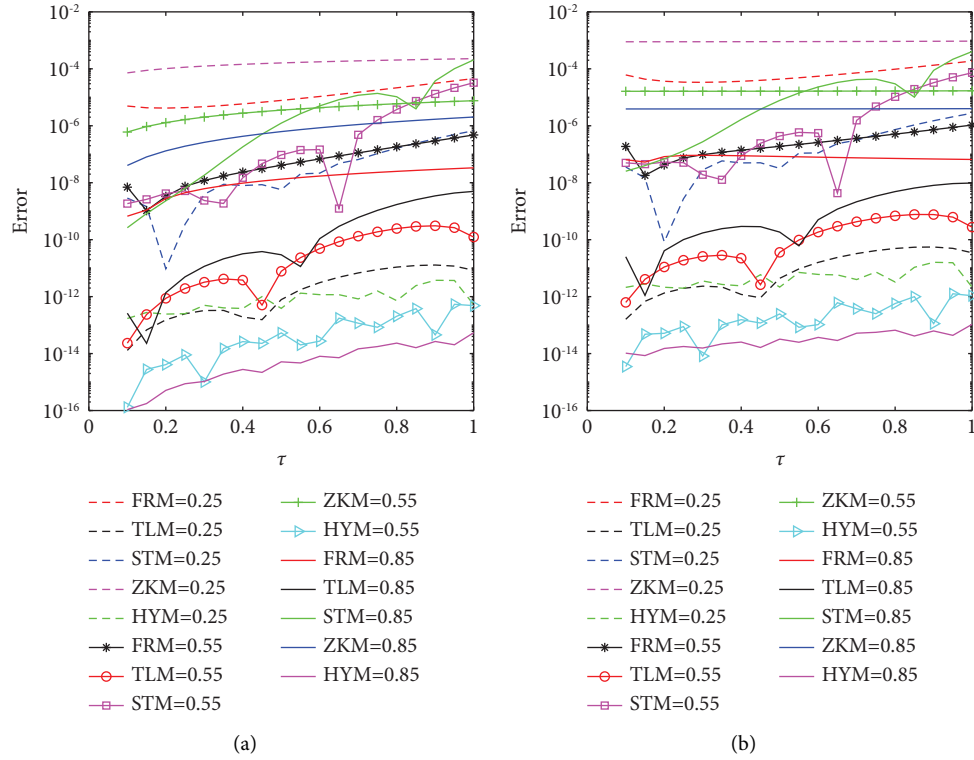


FIGURE 4: (a) The comparison of Ab_{Error} of all the proposed numerical methods for different values of σ and ζ for problem 1; FRM = 0.25, TLM = 0.25, HYM = 0.25, STM = 0.25, ZKM = 0.25 refers to errors of the numerical methods with $\sigma = \zeta = 0.25$. (b) The comparison of RL_{Error} of all the proposed numerical methods for different values of σ and ζ for problem 1; FRM = 0.25, TLM = 0.25, HYM = 0.25, STM = 0.25, ZKM = 0.25 refers to errors of the numerical methods with $\sigma = \zeta = 0.25$.

TABLE 7: The errors obtained using TLM for problem 2 with various values of σ and ζ and $M_T = 24$.

τ	$(\sigma, \zeta) = (0.25, 0.25)$		$(\sigma, \zeta) = (0.55, 0.55)$		$(\sigma, \zeta) = (0.85, 0.85)$	
	Ab_{Error}	RL_{Error}	Ab_{Error}	RL_{Error}	Ab_{Error}	RL_{Error}
0.1	9.4923×10^{-14}	1.4088×10^{-11}	2.3508×10^{-08}	6.8616×10^{-08}	8.5946×10^{-13}	1.2082×10^{-09}
0.2	1.9531×10^{-13}	1.0249×10^{-11}	1.4068×10^{-13}	1.1981×10^{-11}	3.5166×10^{-12}	7.6076×10^{-10}
0.3	2.7848×10^{-12}	7.9550×10^{-11}	1.1978×10^{-11}	4.3538×10^{-10}	1.3962×10^{-11}	1.0108×10^{-09}
0.4	1.0838×10^{-11}	2.0115×10^{-10}	6.7908×10^{-11}	1.3493×10^{-09}	1.5855×10^{-10}	5.2789×10^{-09}
0.5	2.5238×10^{-11}	3.3531×10^{-10}	2.0877×10^{-10}	2.5971×10^{-09}	6.9879×10^{-10}	1.2739×10^{-08}
0.6	3.4870×10^{-11}	3.5268×10^{-10}	3.9359×10^{-10}	3.3404×10^{-09}	6.9879×10^{-09}	2.2011×10^{-08}
0.7	1.2608×10^{-12}	1.0130×10^{-11}	2.3781×10^{-10}	1.4613×10^{-09}	3.6510×10^{-09}	2.6849×10^{-08}
0.8	1.7846×10^{-11}	1.1753×10^{-09}	1.5067×10^{-09}	7.0018×10^{-09}	2.3634×10^{-09}	1.2126×10^{-08}
0.9	6.6769×10^{-10}	3.6922×10^{-09}	7.7091×10^{-09}	2.8018×10^{-08}	1.3553×10^{-08}	5.0638×10^{-08}
1.0	1.7109×10^{-09}	8.0977×10^{-09}	2.3508×10^{-08}	6.8616×10^{-08}	7.3220×10^{-08}	2.0607×10^{-07}

TABLE 8: The errors obtained using the STM for problem 2 with various values of σ and ζ and $M_S = 16$.

τ	$(\sigma, \zeta) = (0.25, 0.25)$		$(\sigma, \zeta) = (0.55, 0.55)$		$(\sigma, \zeta) = (0.85, 0.85)$	
	Ab_{Error}	RL_{Error}	Ab_{Error}	RL_{Error}	Ab_{Error}	RL_{Error}
0.1	2.1562×10^{-10}	3.2001×10^{-08}	1.1250×10^{-09}	4.1075×10^{-07}	2.1032×10^{-09}	2.9566×10^{-06}
0.2	4.1848×10^{-10}	2.1959×10^{-08}	3.8578×10^{-09}	3.2855×10^{-07}	1.0952×10^{-08}	2.3694×10^{-06}
0.3	2.2267×10^{-10}	6.3608×10^{-09}	1.8742×10^{-08}	6.8128×10^{-07}	7.9480×10^{-08}	5.7537×10^{-06}
0.4	2.0180×10^{-09}	3.7452×10^{-08}	2.4650×10^{-07}	4.8981×10^{-06}	1.5868×10^{-06}	5.2834×10^{-05}
0.5	6.6717×10^{-08}	8.8640×10^{-07}	5.0216×10^{-07}	6.2469×10^{-06}	8.8461×10^{-06}	1.6126×10^{-04}
0.6	5.8549×10^{-07}	5.8713×10^{-06}	5.1893×10^{-06}	4.4042×10^{-05}	1.0084×10^{-05}	1.1239×10^{-04}
0.7	2.8326×10^{-06}	2.2759×10^{-05}	4.3135×10^{-05}	2.6505×10^{-04}	1.1404×10^{-04}	8.3860×10^{-04}
0.8	9.2412×10^{-06}	6.0860×10^{-05}	1.6627×10^{-04}	7.7271×10^{-04}	7.1816×10^{-04}	3.6848×10^{-03}
0.9	2.1318×10^{-05}	1.1788×10^{-04}	3.9684×10^{-04}	1.4423×10^{-03}	2.2384×10^{-03}	8.3634×10^{-03}
1.0	3.3033×10^{-05}	1.5635×10^{-04}	5.4484×10^{-04}	1.5903×10^{-03}	4.1982×10^{-03}	1.1816×10^{-02}

TABLE 9: The errors obtained using HYM for problem 2 with various values of σ and ζ and $M_H = 160$.

τ	$(\sigma, \zeta) = (0.25, 0.25)$		$(\sigma, \zeta) = (0.55, 0.55)$		$(\sigma, \zeta) = (0.85, 0.85)$	
	Ab_{Error}	RL_{Error}	Ab_{Error}	RL_{Error}	Ab_{Error}	RL_{Error}
0.1	1.1892×10^{-16}	1.7649×10^{-14}	1.1948×10^{-17}	4.3625×10^{-15}	8.8904×10^{-18}	1.2497×10^{-14}
0.2	5.2032×10^{-16}	2.7303×10^{-14}	3.5656×10^{-17}	3.0367×10^{-15}	1.3694×10^{-17}	2.9624×10^{-15}
0.3	8.7855×10^{-16}	2.5097×10^{-14}	1.0160×10^{-16}	3.6933×10^{-15}	4.3267×10^{-18}	3.1322×10^{-16}
0.4	2.8172×10^{-15}	5.2285×10^{-14}	2.5580×10^{-16}	5.0828×10^{-15}	4.5551×10^{-17}	1.5166×10^{-15}
0.5	5.2805×10^{-15}	7.0157×10^{-14}	4.1121×10^{-16}	5.1154×10^{-15}	3.1802×10^{-17}	5.7974×10^{-16}
0.6	6.7725×10^{-15}	6.8499×10^{-14}	9.3361×10^{-16}	7.9236×10^{-15}	3.3248×10^{-17}	3.7057×10^{-16}
0.7	1.3853×10^{-14}	1.1130×10^{-13}	1.4698×10^{-15}	9.0316×10^{-15}	3.2665×10^{-17}	2.4022×10^{-16}
0.8	2.2417×10^{-14}	1.4763×10^{-13}	2.2241×10^{-15}	1.0336×10^{-14}	3.0069×10^{-17}	1.5428×10^{-16}
0.9	1.7340×10^{-14}	9.5887×10^{-14}	4.5083×10^{-15}	1.6385×10^{-14}	3.6636×10^{-16}	1.3688×10^{-15}
1.0	5.1821×10^{-14}	2.4527×10^{-13}	4.9680×10^{-15}	1.4501×10^{-14}	1.3295×10^{-16}	3.7418×10^{-16}

TABLE 10: The errors obtained using the ZKM for problem 2 with various values of σ and ζ .

τ	$(\sigma, \zeta) = (0.25, 0.25)$		$(\sigma, \zeta) = (0.55, 0.55)$		$(\sigma, \zeta) = (0.85, 0.85)$	
	Ab_{Error}	RL_{Error}	Ab_{Error}	RL_{Error}	Ab_{Error}	RL_{Error}
0.1	6.8875×10^{-08}	1.0222×10^{-05}	9.8134×10^{-10}	3.5830×10^{-07}	1.1462×10^{-10}	1.6113×10^{-07}
0.2	1.9481×10^{-07}	1.0222×10^{-05}	4.2071×10^{-09}	3.5830×10^{-07}	7.4482×10^{-10}	1.6113×10^{-07}
0.3	3.5789×10^{-07}	1.0224×10^{-05}	9.8577×10^{-09}	3.5833×10^{-07}	2.2258×10^{-09}	1.6113×10^{-07}
0.4	5.5100×10^{-07}	1.0226×10^{-05}	1.8036×10^{-08}	3.5838×10^{-07}	4.8398×10^{-09}	1.6114×10^{-07}
0.5	7.7005×10^{-07}	1.0231×10^{-05}	2.8817×10^{-08}	3.5849×10^{-07}	8.8406×10^{-09}	1.6116×10^{-07}
0.6	1.0123×10^{-06}	1.0238×10^{-05}	4.2259×10^{-08}	3.5866×10^{-07}	1.4463×10^{-08}	1.6120×10^{-07}
0.7	1.2756×10^{-06}	1.0249×10^{-05}	5.8412×10^{-08}	3.5892×10^{-07}	2.1929×10^{-08}	1.6126×10^{-07}
0.8	1.5585×10^{-06}	1.0264×10^{-05}	7.7316×10^{-08}	3.5930×10^{-07}	3.1447×10^{-08}	1.6135×10^{-07}
0.9	1.5585×10^{-06}	1.0283×10^{-05}	9.9007×10^{-08}	3.5983×10^{-07}	4.3218×10^{-08}	1.6148×10^{-07}
1.0	2.1781×10^{-06}	1.0309×10^{-05}	1.2352×10^{-07}	3.6053×10^{-07}	5.7436×10^{-08}	1.6165×10^{-07}

TABLE 11: The errors obtained using the FRM for problem 2 with various values of σ and ζ and $T = 4$.

τ	$(\sigma, \zeta) = (0.25, 0.25)$		$(\sigma, \zeta) = (0.55, 0.55)$		$(\sigma, \zeta) = (0.85, 0.85)$	
	Ab_{Error}	RL_{Error}	Ab_{Error}	RL_{Error}	Ab_{Error}	RL_{Error}
0.1	6.0745×10^{-08}	9.0152×10^{-06}	1.0189×10^{-07}	3.7203×10^{-05}	4.4137×10^{-07}	6.2045×10^{-04}
0.2	6.2155×10^{-08}	3.2615×10^{-06}	4.3202×10^{-08}	3.6794×10^{-06}	2.0005×10^{-07}	4.3278×10^{-05}
0.3	6.0687×10^{-08}	1.7336×10^{-06}	2.4251×10^{-08}	8.8154×10^{-07}	8.5220×10^{-08}	6.1692×10^{-06}
0.4	5.7980×10^{-08}	1.0761×10^{-06}	1.0084×10^{-07}	2.0037×10^{-06}	4.1786×10^{-07}	1.3913×10^{-05}
0.5	5.4322×10^{-08}	7.2172×10^{-07}	1.8695×10^{-07}	2.3256×10^{-06}	8.0121×10^{-07}	1.4606×10^{-05}
0.6	4.9781×10^{-08}	5.0350×10^{-07}	2.8292×10^{-07}	2.4012×10^{-06}	1.2384×10^{-06}	1.3803×10^{-05}
0.7	4.4362×10^{-08}	3.5644×10^{-07}	3.8906×10^{-07}	2.3906×10^{-06}	1.7325×10^{-06}	1.2740×10^{-05}
0.8	3.8052×10^{-08}	2.5060×10^{-07}	5.0556×10^{-07}	2.3495×10^{-06}	2.2859×10^{-06}	1.1729×10^{-05}
0.9	3.0829×10^{-08}	1.7048×10^{-07}	6.3257×10^{-07}	2.2990×10^{-06}	2.9011×10^{-06}	1.0839×10^{-05}
1.0	2.2670×10^{-08}	1.0730×10^{-07}	7.7011×10^{-07}	2.2478×10^{-06}	3.5797×10^{-06}	1.0075×10^{-05}

Ab_{Error} and RL_{Error} for various values of σ and ζ using the STM are shown. Figure 11(b) shows the plot of Ab_{Error} and RL_{Error} of ZKM. Similarly in Figure 12(a) a comparison between the Ab_{Error} using the five NILT schemes is

presented and in Figure 12(b) a comparison between the RL_{Error} using the five NILT schemes is presented. It can be seen that the proposed NILT methods have solved the problem with acceptable accuracy.

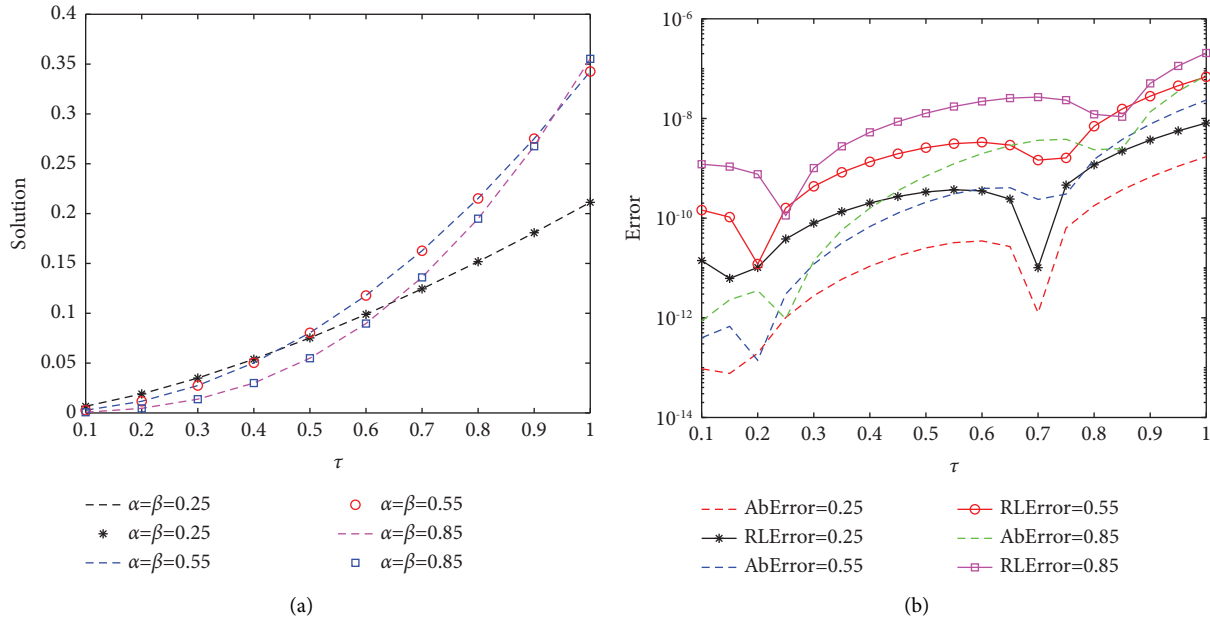


FIGURE 5: (a) The comparison of the numerical solution (dashed lines) and exact solutions (markers) of problem 2 using TLM. (b) The comparison of Ab_{Error} (dashed lines) RL_{Error} (markers) of problem 2 using TLM.

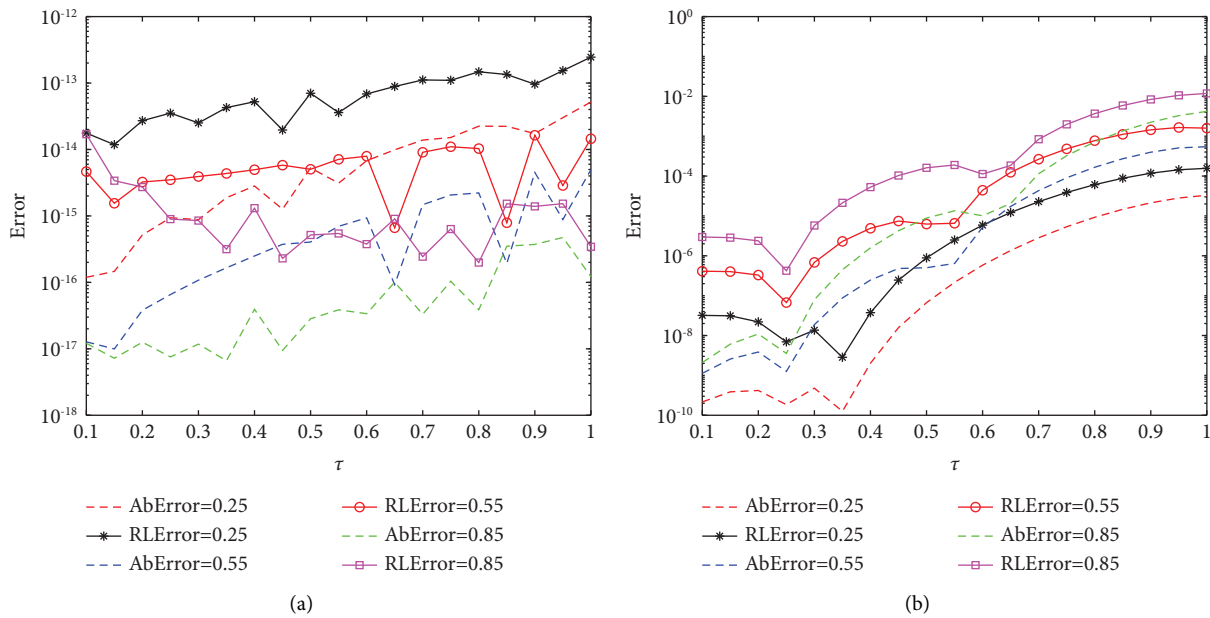


FIGURE 6: (a) The comparison of Ab_{Error} (dashed lines) and RL_{Error} (markers) for problem 2 using HYM. (b) The comparison of Ab_{Error} (dashed lines) and RL_{Error} (markers) for problem 2 using the STM.

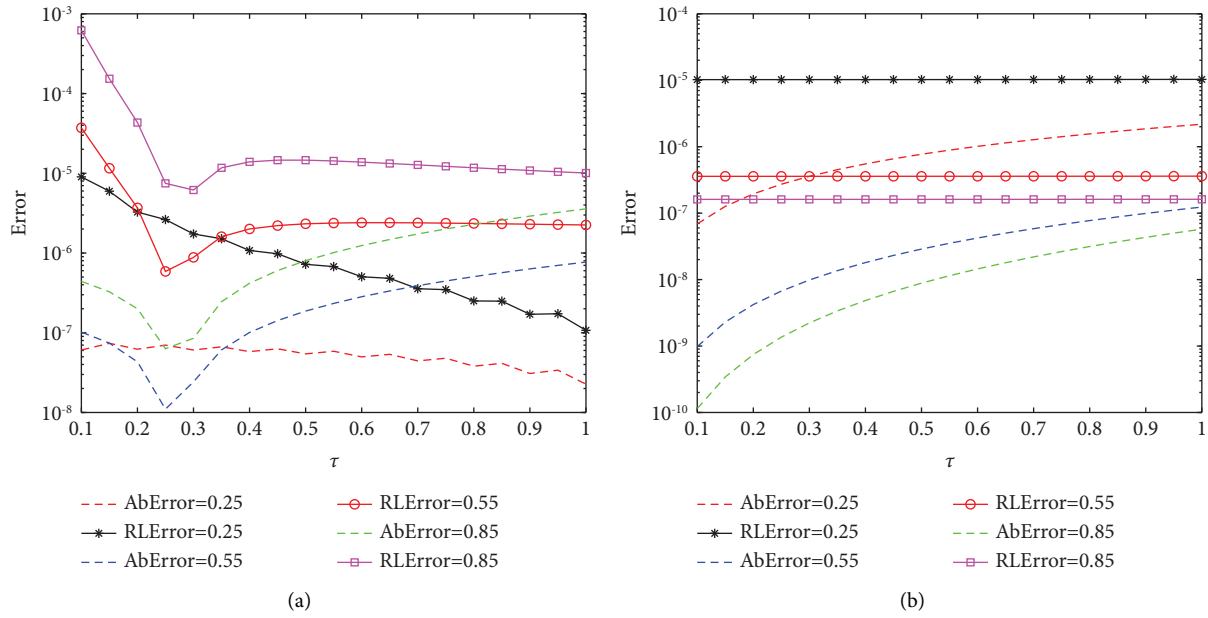


FIGURE 7: (a) The comparison of Ab_{Error} (dashed lines) and RL_{Error} (markers) for problem 2 using the FRM. (b) The comparison of Ab_{Error} (dashed lines) and RL_{Error} (markers) for problem 2 using the ZKM.

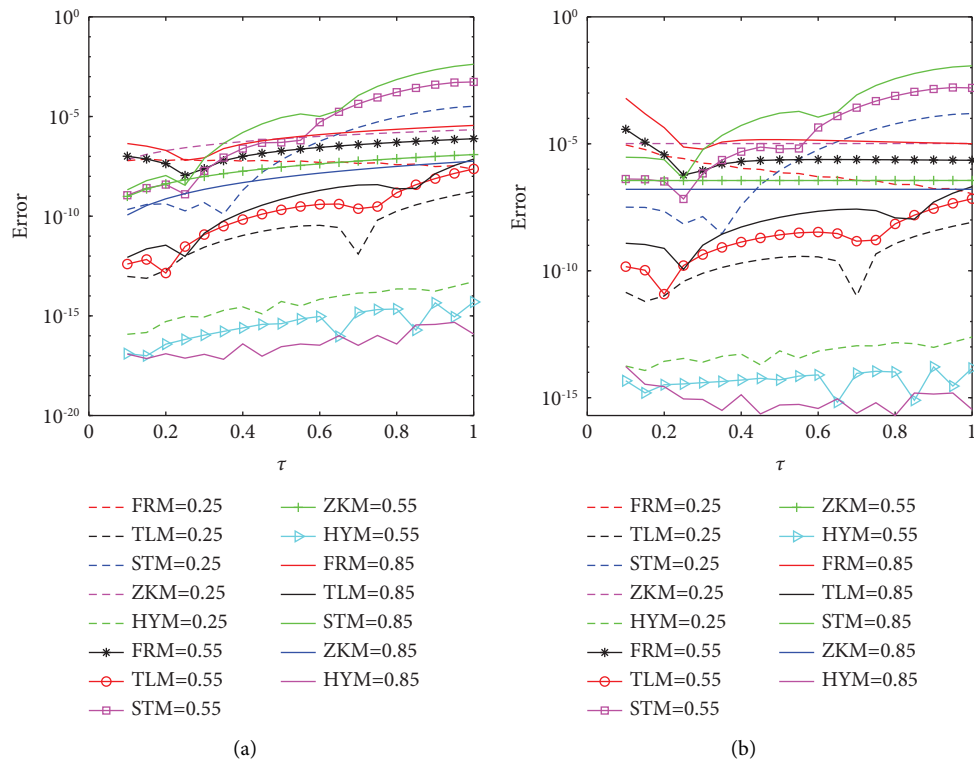


FIGURE 8: (a) The comparison of Ab_{Error} of all the proposed numerical methods for different values of σ and ζ for problem 2; FRM = 0.25, TLM = 0.25, HYM = 0.25, STM = 0.25, ZKM = 0.25 refers to errors of the numerical methods with $\sigma = \zeta = 0.25$. (b) The comparison of RL_{Error} of all the proposed numerical methods for different values of σ and ζ for problem 2; FRM = 0.25, TLM = 0.25, HYM = 0.25, STM = 0.25, ZKM = 0.25 refers to errors of the numerical methods with $\sigma = \zeta = 0.25$.

TABLE 12: The errors obtained using TLM for problem 3 with various values of σ and ζ and $M_T = 24$.

τ	$(\sigma, \zeta) = (0.25, 0.25)$		$(\sigma, \zeta) = (0.55, 0.55)$		$(\sigma, \zeta) = (0.85, 0.85)$	
	Ab_{Error}	RL_{Error}	Ab_{Error}	RL_{Error}	Ab_{Error}	RL_{Error}
0.1	3.7828×10^{-13}	6.2379×10^{-10}	1.0215×10^{-12}	4.5338×10^{-09}	1.6069×10^{-12}	2.9325×10^{-08}
0.2	1.5003×10^{-12}	4.3736×10^{-10}	7.3679×10^{-12}	3.8141×10^{-09}	1.9624×10^{-11}	2.7557×10^{-08}
0.3	4.3562×10^{-12}	4.6082×10^{-10}	1.1628×10^{-12}	1.7127×10^{-10}	5.2105×10^{-11}	1.6323×10^{-08}
0.4	5.8404×10^{-11}	3.0097×10^{-09}	2.1094×10^{-10}	1.2736×10^{-08}	2.1301×10^{-10}	2.3017×10^{-08}
0.5	2.8273×10^{-10}	8.3408×10^{-09}	1.3767×10^{-09}	4.1619×10^{-08}	2.5941×10^{-09}	1.2276×10^{-07}
0.6	9.1242×10^{-10}	1.7066×10^{-08}	5.4734×10^{-09}	9.4033×10^{-08}	1.3521×10^{-08}	3.2593×10^{-07}
0.7	2.1715×10^{-09}	2.7631×10^{-08}	1.5771×10^{-08}	1.6803×10^{-07}	4.9089×10^{-08}	6.6900×10^{-07}
0.8	3.6437×10^{-09}	3.3213×10^{-08}	3.3154×10^{-08}	2.3355×10^{-07}	1.3641×10^{-07}	1.1344×10^{-06}
0.9	2.4551×10^{-09}	1.6678×10^{-08}	4.0360×10^{-08}	1.9741×10^{-07}	2.8779×10^{-07}	1.5481×10^{-06}
1.0	1.0806×10^{-08}	5.6440×10^{-08}	4.3206×10^{-08}	1.5251×10^{-07}	3.8147×10^{-07}	1.3899×10^{-06}

TABLE 13: The errors obtained using the STM for problem 3 with various values of σ and ζ and $M_S = 16$.

τ	$(\sigma, \zeta) = (0.25, 0.25)$		$(\sigma, \zeta) = (0.55, 0.55)$		$(\sigma, \zeta) = (0.85, 0.85)$	
	Ab_{Error}	RL_{Error}	Ab_{Error}	RL_{Error}	Ab_{Error}	RL_{Error}
0.1	1.0479×10^{-09}	1.7280×10^{-06}	1.4789×10^{-09}	6.5642×10^{-06}	1.2707×10^{-10}	2.3189×10^{-06}
0.2	5.4142×10^{-09}	1.5783×10^{-06}	1.6492×10^{-08}	8.5371×10^{-06}	2.3090×10^{-08}	3.2425×10^{-05}
0.3	1.4834×10^{-08}	1.5692×10^{-06}	3.2368×10^{-08}	4.7674×10^{-06}	3.3637×10^{-07}	1.0537×10^{-04}
0.4	5.5227×10^{-07}	2.8460×10^{-05}	4.0370×10^{-06}	2.4374×10^{-04}	7.1192×10^{-06}	7.6926×10^{-04}
0.5	4.5290×10^{-06}	1.3361×10^{-04}	4.1892×10^{-05}	1.2665×10^{-03}	1.2781×10^{-04}	6.0485×10^{-03}
0.6	1.5695×10^{-05}	2.9355×10^{-04}	1.5449×10^{-04}	2.6542×10^{-03}	6.5205×10^{-04}	1.5718×10^{-02}
0.7	4.2928×10^{-06}	5.4622×10^{-05}	9.6189×10^{-06}	1.0249×10^{-04}	9.3686×10^{-04}	1.2768×10^{-02}
0.8	1.9075×10^{-04}	1.7388×10^{-03}	2.1341×10^{-03}	1.5033×10^{-02}	4.8701×10^{-03}	4.0500×10^{-02}
0.9	9.5113×10^{-04}	6.4611×10^{-03}	9.9057×10^{-03}	4.8450×10^{-02}	3.2222×10^{-02}	1.7332×10^{-01}
1.0	2.6710×10^{-03}	1.3951×10^{-02}	2.4489×10^{-02}	8.6443×10^{-02}	9.2725×10^{-02}	3.3784×10^{-01}

TABLE 14: The errors obtained using HYM for problem 3 with various values of σ and ζ and $M_H = 160$.

τ	$(\sigma, \zeta) = (0.25, 0.25)$		$(\sigma, \zeta) = (0.55, 0.55)$		$(\sigma, \zeta) = (0.85, 0.85)$	
	Ab_{Error}	RL_{Error}	Ab_{Error}	RL_{Error}	Ab_{Error}	RL_{Error}
0.1	4.4960×10^{-18}	7.4139×10^{-15}	1.2594×10^{-17}	5.5901×10^{-14}	3.1768×10^{-17}	5.7976×10^{-13}
0.2	3.8148×10^{-18}	1.1120×10^{-15}	1.6549×10^{-17}	8.5667×10^{-15}	2.7217×10^{-17}	3.8219×10^{-14}
0.3	1.3439×10^{-17}	1.4217×10^{-15}	1.9935×10^{-17}	2.9363×10^{-15}	2.5164×10^{-17}	7.8829×10^{-15}
0.4	2.0973×10^{-17}	1.0808×10^{-15}	2.3641×10^{-17}	1.4273×10^{-15}	1.5107×10^{-17}	1.6324×10^{-15}
0.5	4.1922×10^{-17}	1.2367×10^{-15}	9.7941×10^{-18}	2.9609×10^{-16}	1.5593×10^{-17}	7.3794×10^{-16}
0.6	6.2396×10^{-17}	1.1670×10^{-15}	7.2055×10^{-17}	1.2379×10^{-15}	1.3878×10^{-17}	3.3454×10^{-16}
0.7	7.2809×10^{-17}	9.2644×10^{-16}	6.3744×10^{-17}	6.7917×10^{-16}	5.5723×10^{-17}	7.5941×10^{-16}
0.8	1.1414×10^{-16}	1.0405×10^{-15}	1.4043×10^{-16}	9.8925×10^{-16}	8.8175×10^{-17}	7.3326×10^{-16}
0.9	4.7460×10^{-16}	3.2240×10^{-15}	5.6716×10^{-17}	2.7740×10^{-16}	1.4195×10^{-16}	7.6356×10^{-16}
1.0	1.2174×10^{-16}	6.3586×10^{-16}	1.4003×10^{-16}	4.9427×10^{-16}	1.2268×10^{-16}	4.4699×10^{-16}

TABLE 15: The errors obtained using the ZKM for problem 3 with various values of σ and ζ .

τ	$(\sigma, \zeta) = (0.25, 0.25)$		$(\sigma, \zeta) = (0.55, 0.55)$		$(\sigma, \zeta) = (0.85, 0.85)$	
	Ab_{Error}	RL_{Error}	Ab_{Error}	RL_{Error}	Ab_{Error}	RL_{Error}
0.1	2.0469×10^{-10}	3.3754×10^{-07}	6.6460×10^{-13}	2.9499×10^{-09}	6.2603×10^{-13}	1.1425×10^{-08}
0.2	1.1579×10^{-09}	3.3754×10^{-07}	5.6984×10^{-12}	2.9498×10^{-09}	8.1359×10^{-12}	1.1425×10^{-08}
0.3	3.1909×10^{-09}	3.3755×10^{-07}	2.0027×10^{-11}	2.9498×10^{-09}	3.6470×10^{-11}	1.1425×10^{-08}
0.4	6.5502×10^{-09}	3.3755×10^{-07}	4.8857×10^{-11}	2.9498×10^{-09}	1.0573×10^{-10}	1.1425×10^{-08}
0.5	1.1443×10^{-08}	3.3757×10^{-07}	9.7571×10^{-11}	2.9497×10^{-09}	2.4142×10^{-10}	1.1425×10^{-08}
0.6	1.8050×10^{-08}	3.3760×10^{-07}	1.7168×10^{-10}	2.9495×10^{-09}	4.7396×10^{-10}	1.1425×10^{-08}
0.7	2.6537×10^{-08}	3.3766×10^{-07}	2.7679×10^{-10}	2.9491×10^{-09}	8.3836×10^{-10}	1.1425×10^{-08}
0.8	3.7053×10^{-08}	3.3775×10^{-07}	4.1854×10^{-10}	2.9484×10^{-09}	1.3740×10^{-09}	1.1426×10^{-08}
0.9	4.9739×10^{-08}	3.3789×10^{-07}	6.0260×10^{-10}	2.9474×10^{-09}	2.1243×10^{-09}	1.1427×10^{-08}
1.0	6.4727×10^{-08}	3.3808×10^{-07}	8.3456×10^{-10}	2.9458×10^{-09}	3.1366×10^{-09}	1.1428×10^{-08}

TABLE 16: The errors obtained using the FRM for problem 3 with various values of σ and ζ and $T = 4$.

τ	$(\sigma, \zeta) = (0.25, 0.25)$		$(\sigma, \zeta) = (0.55, 0.55)$		$(\sigma, \zeta) = (0.85, 0.85)$	
	Ab_{Error}	RL_{Error}	Ab_{Error}	RL_{Error}	Ab_{Error}	RL_{Error}
0.1	8.9775×10^{-07}	1.4804×10^{-03}	1.8249×10^{-06}	8.1000×10^{-03}	1.1243×10^{-05}	2.0519×10^{-01}
0.2	8.5539×10^{-07}	2.4935×10^{-04}	8.7655×10^{-07}	4.5376×10^{-04}	8.6996×10^{-06}	1.2216×10^{-02}
0.3	7.9431×10^{-07}	8.4026×10^{-05}	2.9870×10^{-07}	4.3995×10^{-05}	5.3294×10^{-06}	1.6695×10^{-03}
0.4	7.1203×10^{-07}	3.6693×10^{-05}	1.7292×10^{-06}	1.0440×10^{-04}	9.9999×10^{-07}	1.0805×10^{-04}
0.5	6.0586×10^{-07}	1.7873×10^{-05}	3.4450×10^{-06}	1.0415×10^{-04}	4.4338×10^{-06}	2.0982×10^{-04}
0.6	4.7300×10^{-07}	8.8468×10^{-06}	5.4771×10^{-06}	9.4097×10^{-05}	1.1129×10^{-05}	2.6828×10^{-04}
0.7	3.1047×10^{-07}	3.9505×10^{-06}	7.8580×10^{-06}	8.3724×10^{-05}	1.9255×10^{-05}	2.6241×10^{-04}
0.8	1.1517×10^{-07}	1.0498×10^{-06}	1.0620×10^{-05}	7.4815×10^{-05}	2.8990×10^{-05}	2.4108×10^{-04}
0.9	1.1613×10^{-07}	7.8890×10^{-07}	1.3798×10^{-05}	6.7485×10^{-05}	4.0525×10^{-05}	2.1799×10^{-04}
1.0	3.8674×10^{-07}	2.0200×10^{-06}	1.7422×10^{-05}	6.1497×10^{-05}	5.4056×10^{-05}	1.9695×10^{-04}

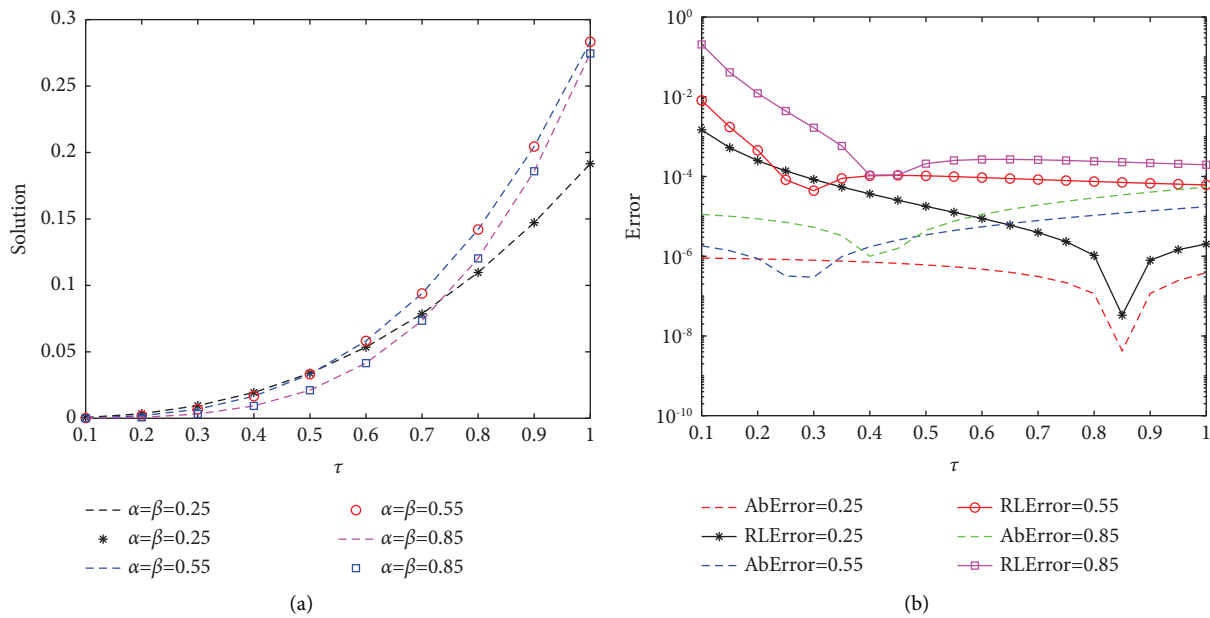


FIGURE 9: (a) The comparison of the numerical solution (dashed lines) and exact solutions (markers) for problem 3 using the FRM. (b) The comparison of Ab_{Error} (dashed lines) and RL_{Error} (markers) for problem 3 using the FRM.

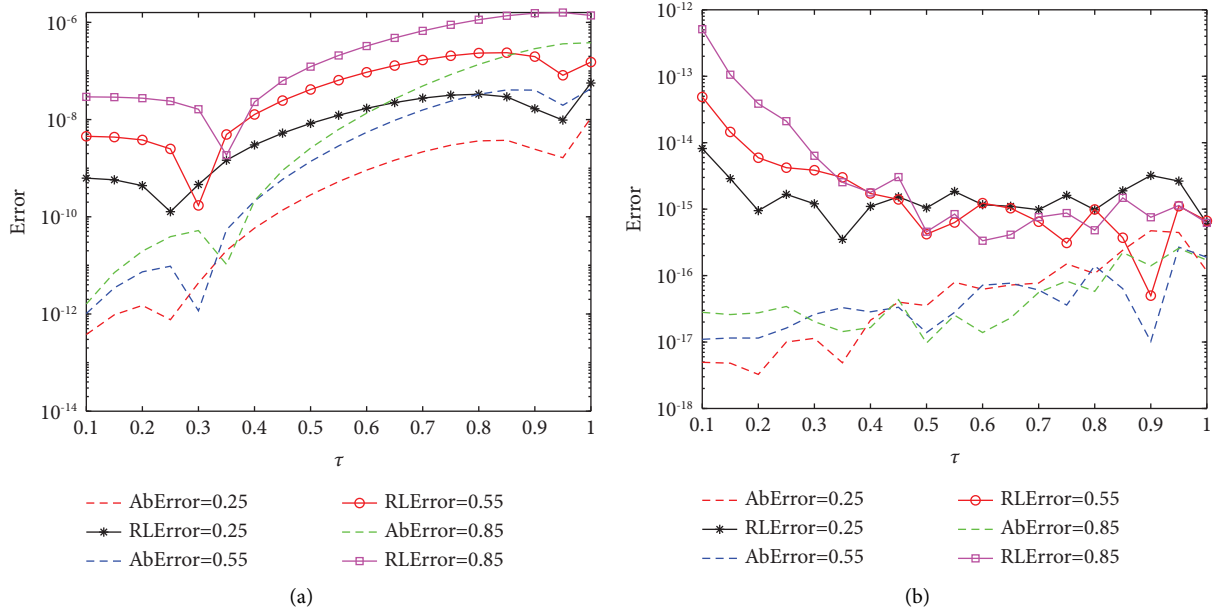


FIGURE 10: (a) The comparison of Ab_{Error} (dashed lines) and RL_{Error} (markers) for problem 4 using TLM. (b) The comparison of Ab_{Error} (dashed lines) and RL_{Error} (markers) for problem 4 using HYM.

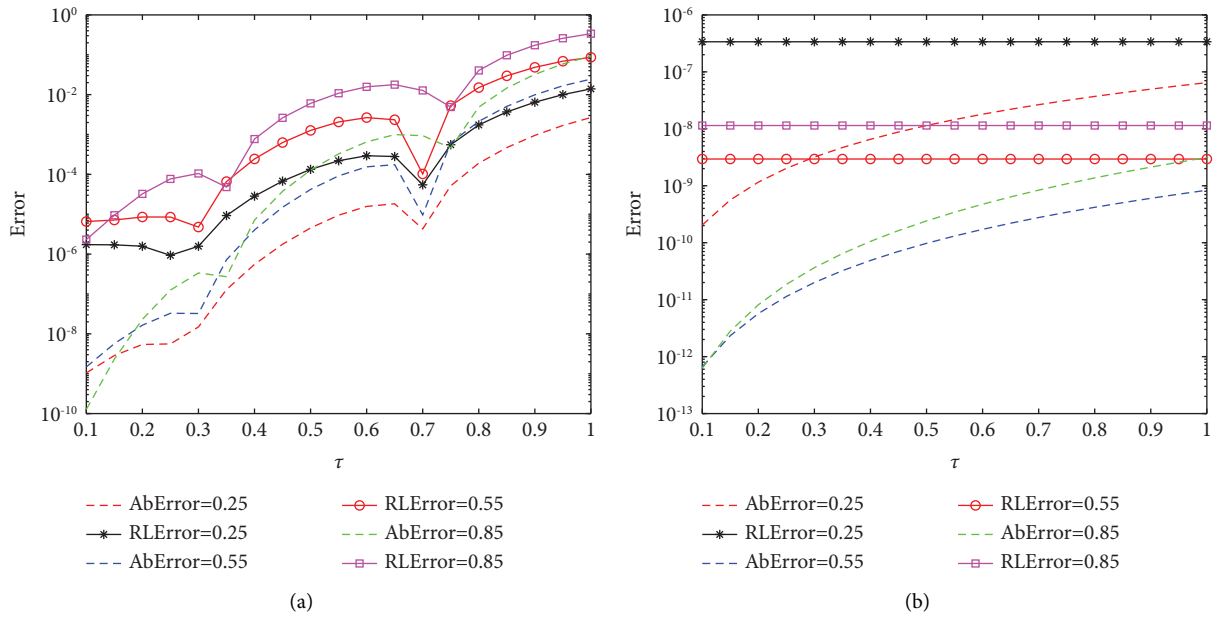


FIGURE 11: (a) The comparison of Ab_{Error} (dashed lines) and RL_{Error} (markers) for problem 4 using the STM. (b) The comparison of Ab_{Error} (dashed lines) and RL_{Error} (markers) for problem 4 using the ZKM.

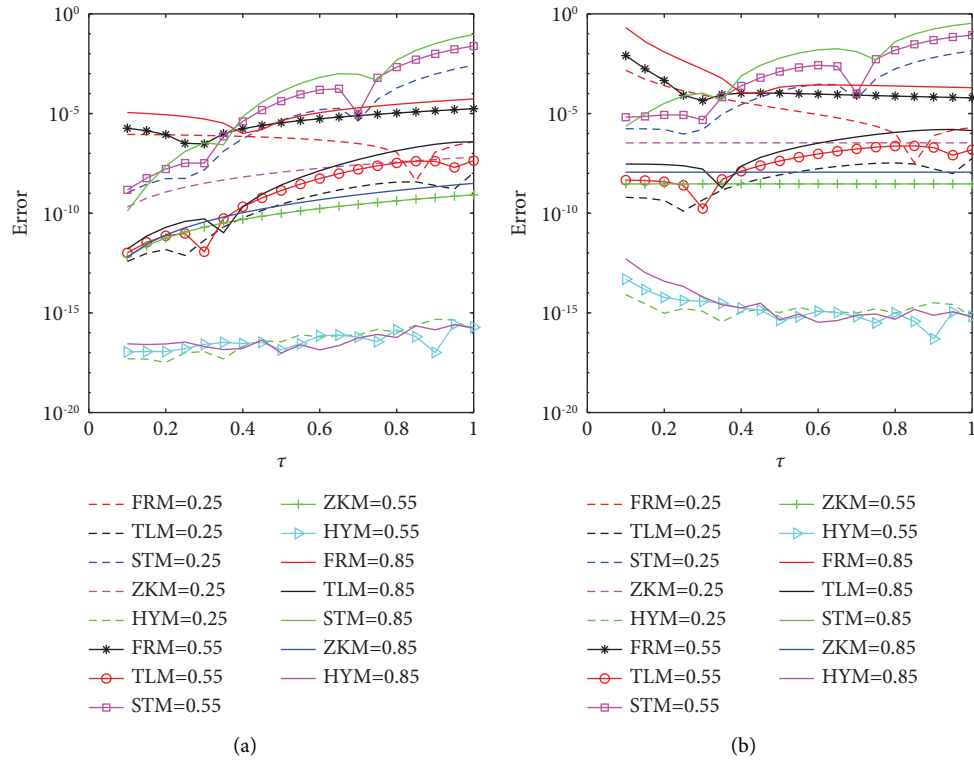


FIGURE 12: (a) The comparison of Ab_{Error} of all the proposed numerical methods for different values of σ and ζ for problem 3; FRM = 0.25, TLM = 0.25, HYM = 0.25, STM = 0.25, ZKM = 0.25 refers to errors of the numerical methods with $\sigma = \zeta = 0.25$. (b) The comparison of RL_{Error} of all the proposed numerical methods for different values of σ and ζ for problem 3; FRM = 0.25, TLM = 0.25, HYM = 0.25, STM = 0.25, ZKM = 0.25 refers to errors of the numerical methods with $\sigma = \zeta = 0.25$.

4. Conclusion

A class of integrodifferential equations with fractal-fractional differential operators has been investigated. The concerned class plays an important role in real-world complex problems. In addition, we have used the properties of the Laplace transform to derive exact solutions of the considered integrodifferential equations under the Caputo fractal-fractional derivative. Moreover, we have obtained the approximate solutions of given integrodifferential equations via numerically inverting the Laplace transform. Here, we remark that for numerical inversion of the Laplace transform, we have evaluated five different numerical schemes. The performance of the proposed numerical schemes has been proven via examples. All the numerical inversion techniques have produced very accurate results. However, it was observed that among all the methods, the contour integration method using the HYM performed better. The results obtained led us to believe that the numerical Laplace inversion techniques often depend on the choice of a free parameter. In addition, it is advantageous to either use more than one inversion technique or perform experimentation and study the effect of the free parameter on the solution. In our future work, we are interested to obtain the exact solution of integrodifferential equations with Caputo–Fabrizio and Atangana–Baleanu fractal-fractional differential operators.

Data Availability

All data required for this research are included within the article.

Conflicts of Interest

The authors declare that they have no conflicts of interest.

Acknowledgments

The authors Kamal Shah, Suhad Subhi Aiadi, and Nabil Mlaiki would like to thank Prince Sultan University for paying the publication fees through TAS research lab, and the author Fahad M. Alotaibi would like to thank the Department of Information Systems, Faculty of Computing and Information Technology (FCIT), King Abdulaziz University, Jeddah 34025, Saudi Arabia. This research was supported by Prince Sultan University, Saudi Arabia.

References

- [1] E. C. De Oliveira and J. A. Tenreiro Machado, “A review of definitions for fractional derivatives and integral,” *Mathematical Problems in Engineering*, vol. 2014, Article ID 238459, 6 pages, 2014.
- [2] J. A. T. M. J. Sabatier, O. P. Agrawal, and J. T. Machado, *Advances in fractional calculus*, Springer, vol. 4, no. 9, Dordrecht, 2007.

- [3] T. Abdeljawad and J. Alzabut, "On Riemann-Liouville fractional q -difference equations and their application to retarded logistic type model," *Mathematical Methods in the Applied Sciences*, vol. 41, no. 18, pp. 8953–8962, 2018.
- [4] J. Alzabut, T. Abdeljawad, F. Jarad, and W. Sudsutad, "A Gronwall inequality via the generalized proportional fractional derivative with applications," *Journal of Inequalities and Applications*, vol. 1, pp. 1–12, 2019.
- [5] N. S. Belevtsov and S. Y. Lukashchuk, "A fast algorithm for fractional Helmholtz equation with application to electromagnetic waves propagation," *Applied Mathematics and Computation*, vol. 416, Article ID 126728, 2022.
- [6] O. Naifar and A. B. Makhlof, *Fractional Order Systems–Control Theory and Applications*, Springer International Publishing, Berlin Germany, 2022.
- [7] M. V. Shitikova, "Fractional operator viscoelastic models in dynamic problems of mechanics of solids: a review," *Mechanics of Solids*, vol. 57, pp. 1–33, 2022.
- [8] Y. Wang and G. Zhao, "A comparative study of fractional-order models for lithium-ion batteries using Runge Kutta optimizer and electrochemical impedance spectroscopy," *Control Engineering Practice*, vol. 133, Article ID 105451, 2023.
- [9] C. Ionescu, A. Lopes, D. Copot, J. T. Machado, and J. H. Bates, "The role of fractional calculus in modeling biological phenomena: a review," *Communications in Nonlinear Science and Numerical Simulation*, vol. 51, pp. 141–159, 2017.
- [10] Q. Yang, D. Chen, T. Zhao, and Y. Chen, "Fractional calculus in image processing: a review," *Fractional Calculus and Applied Analysis*, vol. 19, no. 5, pp. 1222–1249, 2016.
- [11] A. El-Ajou, Z. Odibat, S. Momani, and A. Alawneh, "Construction of analytical solutions to fractional differential equations using homotopy analysis method," *IAENG International Journal of Applied Mathematics*, vol. 40, no. 2, 2010.
- [12] V. Gill, K. Modi, and Y. Singh, "Analytic solutions of fractional differential equation associated with RLC electrical circuit," *Journal of Statistics and Management Systems*, vol. 21, no. 4, pp. 575–582, 2018.
- [13] H. Jaradat, F. Awawdeh, and E. A. Rawashdeh, "Analytic solution of fractional integro-differential equations," *Annals of the University of Craiova - Mathematics and Computer Science Series*, vol. 38, no. 1, pp. 1–10, 2011.
- [14] G. M. Ismail, H. R. Abdl-Rahim, A. Abdel-Aty, R. Kharabsheh, W. Alharbi, and M. Abdel-Aty, "An analytical solution for fractional oscillator in a resisting medium," *Chaos, Solitons and Fractals*, vol. 130, Article ID 109395, 2020.
- [15] M. Senol, "New analytical solutions of fractional symmetric regularized-long-wave equation," *Revista Mexicana de Física*, vol. 66, no. 3, pp. 297–307, 2020.
- [16] W. Malesza, M. Macias, and D. Sierociuk, "Analytical solution of fractional variable order differential equations," *Journal of Computational and Applied Mathematics*, vol. 348, pp. 214–236, 2019.
- [17] J. G. Liu, X. J. Yang, and Y. Y. Feng, "Analytical solutions of some integral fractional differential-difference equations," *Modern Physics Letters B*, vol. 34, no. 1, Article ID 2050009, 2020.
- [18] K. Shah, H. Khalil, and R. A. Khan, "Analytical solutions of fractional order diffusion equations by natural transform method," *Iranian Journal of Science and Technology Transaction A-Science*, vol. 42, no. 3, pp. 1479–1490, 2018.
- [19] Q. Al-Mdallal, K. A. Abro, and I. Khan, "Analytical solutions of fractional Walter's B fluid with applications," *Complexity*, vol. 2018, Article ID 8131329, 10 pages, 2018.
- [20] B. Abdalla, K. Abodayeh, T. Abdeljawad, and J. Alzabut, "New oscillation criteria for forced nonlinear fractional difference equations," *Vietnam Journal of Mathematics*, vol. 45, pp. 609–618, 2017.
- [21] X. Li, Kamran, A. U. Haq, and X. Zhang, "Numerical solution of the linear time fractional Klein-Gordon equation using transform based localized RBF method and quadrature," *AIMS Mathematics*, vol. 5, no. 5, pp. 5287–5308, 2020.
- [22] J. Li, L. Dai, Kamran, and W. Nazeer, "Numerical solution of multi-term time fractional wave diffusion equation using transform based local meshless method and quadrature," *AIMS Mathematics*, vol. 5, no. 6, pp. 5813–5839, 2020.
- [23] Y. Y. Gambo, R. Ameen, F. Jarad, and T. Abdeljawad, "Existence and uniqueness of solutions to fractional differential equations in the frame of generalized Caputo fractional derivatives," *Advances in Difference Equations*, vol. 2018, pp. 1–13, 2018.
- [24] X. Liu, F. Li, M. Jia, and E. Zhi, "Existence and uniqueness of the solutions for fractional differential equations with nonlinear boundary conditions," *Abstract and Applied Analysis*, vol. 2014, Article ID 758390, 11 pages, 2014.
- [25] S. Abbas, "Existence of solutions to fractional order ordinary and delay differential equations and applications," *The Electronic Journal of Differential Equations*, vol. 2011, no. 9, pp. 1–11, 2011.
- [26] J. Wu and Y. Liu, "Existence and uniqueness of solutions for the fractional integro-differential equations in Banach spaces," *The Electronic Journal of Differential Equations*, vol. 129, pp. 1–8, 2009.
- [27] A. Hamoud and K. Ghadle, "Existence and uniqueness of solutions for fractional mixed Volterra-Fredholm integro-differential equations," *Indian Journal of Mathematics*, vol. 60, no. 3, pp. 375–395, 2018.
- [28] S. K. Ntouyas and M. E. Samei, "Existence and uniqueness of solutions for multi-term fractional q -integro-differential equations via quantum calculus," *Advances in Difference Equations*, vol. 2019, no. 1, pp. 1–20, 2019.
- [29] Y. Li and N. Sun, "Numerical solution of fractional differential equations using the generalized block pulse operational matrix," *Computers and Mathematics with Applications*, vol. 62, no. 3, pp. 1046–1054, 2011.
- [30] S. Esmaeili, M. Shamsi, and Y. Luchko, "Numerical solution of fractional differential equations with a collocation method based on Müntz polynomials," *Computers and Mathematics with Applications*, vol. 62, no. 3, pp. 918–929, 2011.
- [31] N. A. Zabidi, Z. A. Majid, A. Kilicman, and Z. B. Ibrahim, "Numerical solution of fractional differential equations with Caputo derivative by using numerical fractional predict-correct technique," *Advances in Continuous and Discrete Models*, vol. 2022, no. 1, pp. 1–23, 2022.
- [32] Y. Y. Yameni Noupoue, Y. Tandoğdu, and M. Awadalla, "On numerical techniques for solving the fractional logistic differential equation," *Advances in Difference Equations*, vol. 2019, no. 1, pp. 1–13, 2019.
- [33] J. Wang, Kamran, A. Jamal, and X. Li, "Numerical solution of fractional-order Fredholm integrodifferential equation in the sense of Atangana-Baleanu derivative," *Mathematical Problems in Engineering*, vol. 2021, Article ID 6662808, 8 pages, 2021.
- [34] X. Qiang, Kamran, A. Mahboob, and Y. M. Chu, "Numerical approximation of fractional-order Volterra integrodifferential equation," *Journal of Function Spaces*, vol. 2020, Article ID 8875792, 12 pages, 2020.

- [35] O. A. Arqub and B. Maayah, "Fitted fractional reproducing kernel algorithm for the numerical solutions of ABC-Fractional Volterra integro-differential equations," *Chaos, Solitons and Fractals*, vol. 126, pp. 394–402, 2019.
- [36] A. Atangana, "Fractal-fractional differentiation and integration: connecting fractal calculus and fractional calculus to predict complex system," *Chaos, Solitons and Fractals*, vol. 102, pp. 396–406, 2017.
- [37] A. Atangana and A. Akgül, "On solutions of fractal fractional differential equations," *Discrete and Continuous Dynamical Systems-S*, vol. 14, no. 10, p. 3441, 2021.
- [38] S. İ. Araz, "Numerical analysis of a new volterra integro-differential equation involving fractal-fractional operators," *Chaos, Solitons and Fractals*, vol. 130, Article ID 109396, 2020.
- [39] S. İ. Araz, "New class of volterra integro-differential equations with fractal-fractional operators: existence, uniqueness and numerical scheme," *Discrete and Continuous Dynamical Systems - Series S*, vol. 14, no. 7, 2021.
- [40] Kamran, S. Ahmad, K. Shah, T. Abdeljawad, and B. Abdalla, "On the approximation of fractal-fractional differential equations using numerical inverse Laplace transform methods," *Computer Modeling in Engineering and Sciences*, vol. 135, no. 3, pp. 2743–2765, 2022.
- [41] K. A. Abro and A. Atangana, "Mathematical analysis of memristor through fractal-fractional differential operators: a numerical study," *Mathematical Methods in the Applied Sciences*, vol. 43, no. 10, pp. 6378–6395, 2020.
- [42] A. Atangana, A. Akgül, and K. M. Owolabi, "Analysis of fractal fractional differential equations," *Alexandria Engineering Journal*, vol. 59, no. 3, pp. 1117–1134, 2020.
- [43] A. A. Kilbas, M. Saigo, and R. K. Saxena, "Generalized Mittag-Leffler function and generalized fractional calculus operators," *Integral Transforms and Special Functions*, vol. 15, no. 1, pp. 31–49, 2004.
- [44] A. Talbot, "The accurate numerical inversion of Laplace transforms," *IMA Journal of Applied Mathematics*, vol. 23, no. 1, pp. 97–120, 1979.
- [45] J. A. C. Weideman, "Improved contour integral methods for parabolic PDEs," *IMA Journal of Numerical Analysis*, vol. 30, no. 1, pp. 334–350, 2010.
- [46] W. McLean and V. Thomée, "Numerical solution via Laplace transforms of a fractional order evolution equation," *Journal of Integral Equations and Applications*, vol. 5794 pages, 2010.
- [47] B. Dingfelder and J. A. C. Weideman, "An improved Talbot method for numerical Laplace transform inversion," *Numerical Algorithms*, vol. 68, no. 1, pp. 167–183, 2015.
- [48] D. P. Gaver, "Observing stochastic processes, and approximate transform inversion," *Operations Research*, vol. 14, no. 3, pp. 444–459, 1966.
- [49] H. Stehfest, "Algorithm 368: numerical inversion of Laplace transforms [D5]," *Communications of the ACM*, vol. 13, no. 1, pp. 47–49, 1970.
- [50] A. Kuznetsov, "On the convergence of the gaver–stehfest algorithm," *SIAM Journal on Numerical Analysis*, vol. 51, no. 6, pp. 2984–2998, 2013.
- [51] B. Davies and B. Martin, "Numerical inversion of the Laplace transform: a survey and comparison of methods," *Journal of Computational Physics*, vol. 33, no. 1, pp. 1–32, 1979.
- [52] J. Abate and W. Whitt, "A unified framework for numerically inverting Laplace transforms," *INFORMS Journal on Computing*, vol. 18, no. 4, pp. 408–421, 2006.
- [53] J. Abate and P., P. Valkó, "Multi-precision Laplace transform inversion," *International Journal for Numerical Methods in Engineering*, vol. 60, no. 5, pp. 979–993, 2004.
- [54] Z. J. Fu, W. Chen, and H. T. Yang, "Boundary particle method for Laplace transformed time fractional diffusion equations," *Journal of Computational Physics*, vol. 235, pp. 52–66, 2013.
- [55] V. Zakian, "Numerical inversion of Laplace transform," *Electronics Letters*, vol. 5, no. 6, pp. 120–121, 1969.
- [56] D. J. Halsted and D. E. Brown, "Zakian's technique for inverting Laplace transforms," *The Chemical Engineering Journal*, vol. 3, pp. 312–313, 1972.
- [57] H. Dubner and J. Abate, "Numerical inversion of Laplace transforms by relating them to the finite Fourier cosine transform," *Journal of the ACM*, vol. 15, no. 1, pp. 115–123, 1968.
- [58] K. S. Crump, "Numerical inversion of Laplace transforms using a Fourier series approximation," *Journal of the ACM*, vol. 23, no. 1, pp. 89–96, 1976.